THE JOURNAL OF BIOLOGICAL CHEMISTRY VOL. 292, NO. 9, pp. 3751–3767, March 3, 2017

Zinc and Copper Differentially Modulate Amyloid Precursor Protein Processing by γ-Secretase and Amyloid-β Peptide Production*[S]

Received for publication, August 17, 2016, and in revised form, January 13, 2017 Published, JBC Papers in Press, January 17, 2017, DOI 10.1074/jbc.M116.754101

Hermeto Gerber[‡§¶1], **Fang Wu**[§‖1], **Mitko Dimitrov**[§], **Guillermo M. Garcia Osuna**[§], **and Patrick C. Fraering**[‡§2]

From the [‡]*Foundation Eclosion, CH-1228 Plan-Les-Ouates, and Campus Biotech Innovation Park, CH-1202 Geneva, Switzerland, the* [§]*Brain Mind Institute and School of Life Sciences, Swiss Federal Institute of Technology (EPFL), CH-1015 Lausanne, Switzerland, the* [¶]*Department of Biology, University of Fribourg, CH-1700 Fribourg, Switzerland, and the* [‖]*Key Laboratory of Systems Biomedicine, Ministry of Education, Shanghai Center for Systems Biomedicine, Shanghai Jiao Tong University, 200240 Shanghai, China*

Edited by Paul E. Fraser

Recent evidence suggests involvement of biometal homeostasis in the pathological mechanisms in Alzheimer's disease (AD). For example, increased intracellular copper or zinc has been linked to a reduction in secreted levels of the AD-causing amyloid-β peptide (Aβ). However, little is known about whether these biometals modulate the generation of Aβ. In the present study we demonstrate in both cell-free and cell-based assays that zinc and copper regulate Aβ production by distinct molecular mechanisms affecting the processing by γ-secretase of its Aβ precursor protein substrate APP-C99. We found that Zn^{2+} induces APP-C99 dimerization, which prevents its cleavage by γ-secretase and Aβ production, with an IC_{50} value of 15 μM. Importantly, at this concentration, Zn^{2+} also drastically raised the production of the aggregation-prone Aβ43 found in the senile plaques of AD brains and elevated the Aβ43:Aβ40 ratio, a promising biomarker for neurotoxicity and AD. We further demonstrate that the APP-C99 histidine residues His-6, His-13, and His-14 control the Zn^{2+}-dependent APP-C99 dimerization and inhibition of Aβ production, whereas the increased Aβ43:Aβ40 ratio is substrate dimerization-independent and involves the known Zn^{2+} binding lysine Lys-28 residue that orientates the APP-C99 transmembrane domain within the lipid bilayer. Unlike zinc, copper inhibited Aβ production by directly targeting the subunits presenilin and nicastrin in the γ-secretase complex. Altogether, our data demonstrate that zinc and copper differentially modulate Aβ production. They further suggest that dimerization of APP-C99 or the specific targeting of individual residues regulating the production of the long, toxic Aβ species, may offer two therapeutic strategies for preventing AD.

Alzheimer's disease (AD)[3] is a neurodegenerative disorder and the most common form of dementia (1). AD is characterized by the cerebral deposition of extracellular amyloid-β (Aβ) plaques and formation of intracellular Tau-enriched neurofibrillary tangles, which together lead to neuronal death and to dementia (2). Although the causal link of the two hallmarks still remains under debate, mainly because the pathogenesis of AD seems to be multifactorial, a growing body of genetic and biochemical evidence supports the Aβ and Tau cascade hypothesis (2). Consequently, different Aβ and Tau-based therapeutic approaches are currently under clinical or preclinical studies for preventing or slowing down the progression of AD (3).

Interestingly, the neuritic plaques found in the brain of AD patients are not exclusively made of Aβ peptides but also contain several other proteins and biometals including up to millimolar concentrations of Cu^{2+} and Zn^{2+} (4, 5). In the synaptic clefts, the concentrations of free Cu^{2+} and Zn^{2+} can, respectively, reach up to ~15 and 300 μM (6–9). Different cell-based and cell-free studies have demonstrated that Cu^{2+} and Zn^{2+} bind Aβ peptides and the amyloid precursor protein (APP) with high affinity (10–12) and are involved in the aggregation or fibrillization of Aβ (10, 13). Further supporting the interplay of Cu^{2+} and APP, overexpression of APP, which harbors a HXH Cu^{2+} or Zn^{2+} binding motif, has been reported to decrease the concentration of intracellular Cu^{2+} in cells and in transgenic AD mice (14, 15). Consistently, knock-out of APP increased cellular Cu^{2+} in primary mouse cortical neurons (16). Moreover, the elevation of intracellular Cu^{2+} or Zn^{2+} levels by genetic or pharmacological methods in different cellular and *in vivo* systems have consistently been shown to attenuate the pro-

* This work was supported by the Swiss National Science Foundation (to H. G. and P. C. F., 31003A_152677/1), the Strauss Foundation (to H. G. and P. C. F.), the Foundation Eclosion (to H. G. and P. C. F.), and the National Natural Science Foundation of China (to F. W., 31270853). The authors declare that they have no conflicts of interest with the contents of this article.

[S] This article contains supplemental Fig. 1–5.

[1] Both authors contributed equally to the work.

[2] To whom correspondence should be addressed. Tel.: 0041-78-640-64-62; Fax: 0041-22-880-10-13; E-mail: fraeringpatrick@hotmail.com.

[3] The abbreviations used are: AD, Alzheimer's disease; Aβ, amyloid-β peptide; aa, amino acid; AICD, amyloid-β precursor protein intracellular domain; Aph1, anterior pharynx-defective 1; APP, amyloid-β precursor protein; rAPP, recombinant APP; APP-CTF, APP-C-terminal fragment; APP-C83, APP C-terminal 83-aa fragment; APP-C99, APP C-terminal 99-aa fragment; Bis-tris, 2-[bis(2-hydroxyethyl)amino]-2-(hydroxymethyl)propane-1,3-diol; CHAPSO, 3-[(3-cholamidopropyl)dimethylammonio]-2-hydroxy-1-propanesulfonic acid; DAPT, *N*-[*N*-(3,5-difluorophenylacetyl)-L-alanyl]-(*S*)-phenylglycine-*t*-butyl ester; DSS, disuccinimidyl suberate; IP, immunoprecipitation; NCT, nicastrin; Pen2, presenilin enhancer 2; PS1, presenilin-1; PS-NTF, presenilin N-terminal fragment; NICD, notch intracellular domain; TMD, transmembrane domain; WD, Wilson disease; ZnT3, zinc transporter-3.

duction of Aβ (17–19). Consistent with that observation, chemical metal chelators, redistributing Cu^{2+} or Zn^{2+} from the extracellular to the intracellular space, reduced Aβ levels in AD mouse models and human clinical studies (2, 20, 21). Yet another study showed that the cortical levels of zinc transporter-3 (ZnT3) are reduced in AD patients and that an "Alzheimer's disease-like" cognitive loss is observed in ZnT3 KO mice (22). Altogether, these cellular and physiological observations strongly indicate that Cu^{2+} and Zn^{2+} homeostasis play important roles in Aβ production, aggregation, and AD pathology.

Interestingly, various mechanisms have been proposed to explain the link between increased intracellular copper/zinc and reduction of secreted Aβ levels, including altered expression (23), trafficking, and processing of APP or induction of Aβ clearance enzymes (24). However, little is known about whether biometals modulate the generation of Aβ from the APP-C-terminal fragment upon its cleavage by the multisubunit protease γ-secretase.

Here we report that Cu^{2+} inhibits the cleavage of the substrates APP-C99, APP-C83, and Notch by binding to the γ-secretase complex. In contrast, high concentrations of zinc completely blocked the proteolytic cleavage by γ-secretase of APP-C99 (but not APP-C83 or Notch) by binding to the histidine residues His-6, His-13, and His-14 and promoting the formation of substrate dimers and higher oligomers. Importantly, Zn^{2+} specifically shifts Aβ production toward Aβ43 by binding to the residue Lys-28 implicated in the orientation of the APP-TMD in the lipid membrane.

Results

Copper and Zinc Inhibit the Processing by γ-Secretase of APP-C99 in Cell-free and Cell-based Assays—The proteolytic processing of APP by the α-secretases ADAM10/17 or the β-secretase BACE1 (two members of the "sheddase" family of membrane-bound proteases cleaving the extracellular portion of type-I transmembrane protein receptors) led to the formation of 83- and 99-aa-long membrane-bound APP-CTFs, respectively (Fig. 1*A*). Although APP-C83 is further processed by γ-secretase to generate the peptides p3 of largely unknown functions, γ-secretase processing of APP-C99 led to the generation of soluble Aβ peptides forming the toxic oligomers, fibrils, and plaques implicated in the pathogenesis of Alzheimer's disease (Fig. 1*A*). In this study we first tested the inhibitory effect of different biometals on APP-C99 processing by a well defined γ-secretase cell-free assay performed with highly purified enzyme and recombinant substrate (rAPP-C99). We found that, in contrast to Li^{+}, Mg^{2+}, Co^{2+}, Mn^{2+}, Ca^{2+}, Ni^{2+}, and Cd^{2+}, which did not affect APP-C99 processing by purified γ-secretase, Cu^{2+} and Zn^{2+} showed a strong inhibitory effect at 10 μM (Fig. 1*B*). Refined analyses revealed that Cu^{2+} and Zn^{2+} inhibited the processing of APP-C99 and the production of AICD and Aβ in a dose-dependent manner (Fig. 1*C*). The physiologic relevance of these observations lays on the availability of Cu^{2+} and Zn^{2+} in the intracellular organelles where γ-secretase processes most of the substrate APP-C99, including the early and late endosomal vesicles (25, 26). Indeed, it has been demonstrated that the concentrations of Cu^{2+} and Zn^{2+} can reach extracellularly up to 300 μM in the neuronal synaptic clefts (6–9) but that only a small percentage of Aβ is produced at the plasma membrane (25, 26). Yet immunocytochemical studies have demonstrated that copper transporters are localized at the plasma membrane in HEK293 human embryonic kidney cells (27), which facilitates copper uptake across the plasma membrane and potential exposure to γ-secretase and the substrate APP-C99. In other cells such as HeLa, these transporters are predominantly localized to vesicular compartments (27). Because of these observations, we first investigated the effects of both Cu^{2+} and Zn^{2+} on the processing of APP in human embryonic kidney (HEK 293T) cells transiently transfected with APP-C99. In those cells we found that Cu^{2+} and Zn^{2+} treatments caused an accumulation of APP-CTFs that correlated with reduced Aβ production with relative half-maximal inhibitory concentration (IC_{50}) values of ~70 μM and ~20 μM, respectively (Fig. 1*D*). Very similar effects were found for both cupric (Cu^{2+}) and cuprous (Cu^{+}) copper (supplemental Fig. S1), which are the two major oxidation states for this metal present in the human body and in cells (28). It indicates that γ-secretase inhibition is independent of the oxidation state of this metal. Because *in vitro* and *in vivo* experiments have shown that kainite receptor activation facilitates zinc influx into neuronal cells (29, 30), we next investigated the effects of both Zn^{2+} and Cu^{2+} on the processing of APP in rat primary cortical neurons activated for 24 h with 30 μM of kainic acid. In those cells we found that Zn^{2+} and Cu^{2+} treatments caused a dose-dependent accumulation of APP-CTFs, most likely caused by altered substrate processing by γ-secretase, without affecting cell viability (Fig. 1*E*). Endogenous Aβ1–40 levels were below detection limits.

Altogether, our results show that Zn^{2+} and Cu^{2+} treatments of HEK and neuronal cells affect APP processing and Aβ production, further supporting previous studies, showing that exposure to copper and genetic or pharmacological elevation of intracellular copper levels in different cell culture models and AD mouse models decrease Aβ production (17–19, 24, 31–33).

Copper Inhibits the Processing by γ-Secretase of APP and Notch without Affecting the Substrate Quaternary Structure—Before the cell-free γ-secretase activity assays, the APP-C99 substrate purified from *Escherichia coli* was incubated with 0.5% SDS for 5 min at 65 °C and further centrifuged for 1 min at 11,000 × *g*. This preclearing treatment allowed for the separation between the aggregated substrates and the monomeric, native APP-C99 substrates, the latter of which are the species processed by the purified γ-secretase complex. Analysis by SDS-PAGE of the precleared substrate revealed a protein migrating at the size expected for a monomeric species (Fig. 2*A*). We further characterized the species found in the precleared substrate preparation under native (non-SDS) conditions. To address this question, we followed a cross-linking approach by using the well known amine-reactive chemical cross-linker disuccinimidyl suberate (DSS), which allows for the covalent bridging of native oligomeric species present in the solution. Thus, SDS-PAGE analysis of the cross-linked species reveals the identity of the native quaternary structural species found in the substrate solution. As shown in Fig. 2*B*, we found that almost all of the precleared APP-C99 substrate adopts a monomeric structure; only traces of residual dimers of APP-

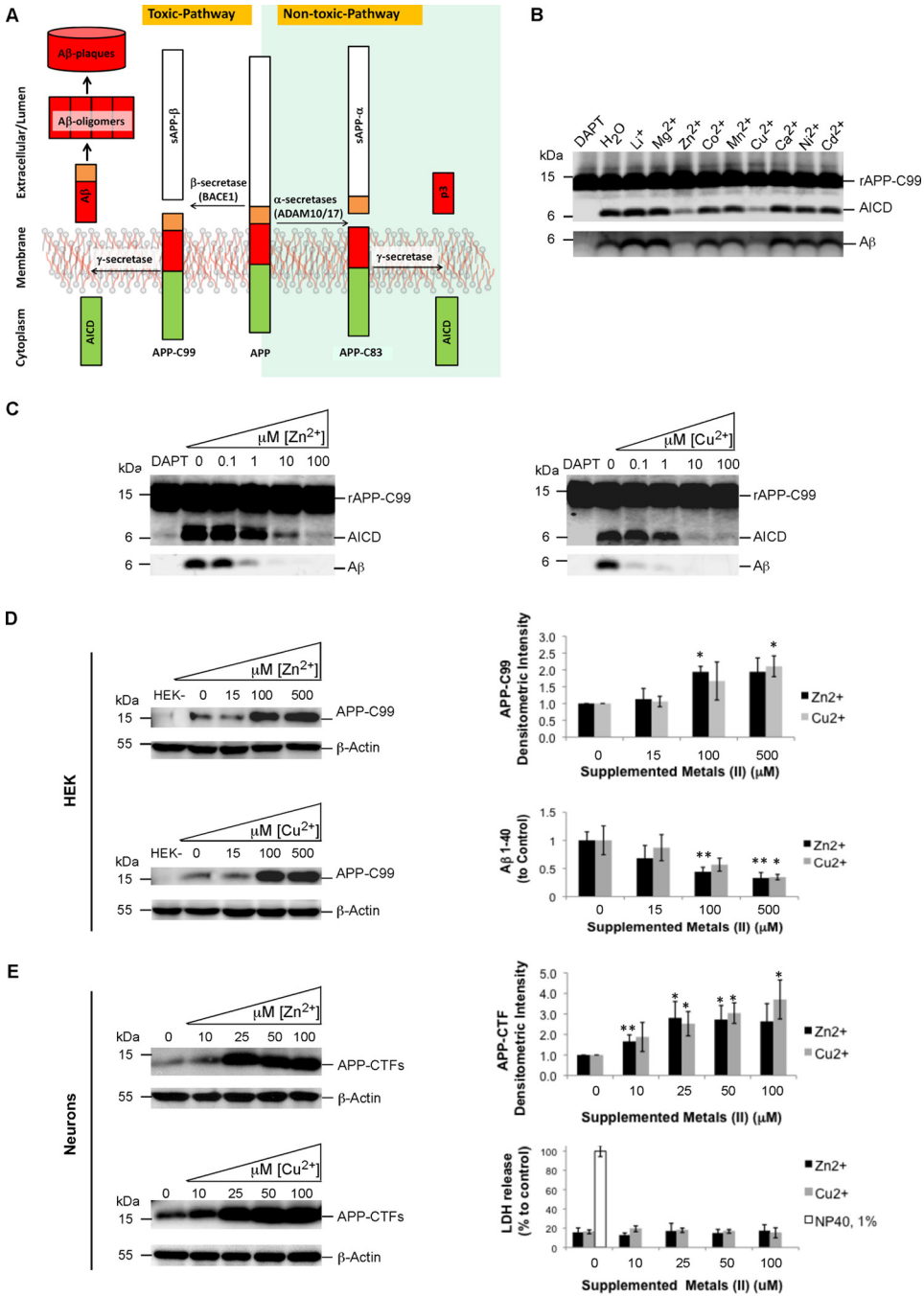

FIGURE 1. **Zn^{2+} and Cu^{2+} inhibit the proteolytic processing of APP by γ-secretase.** *A*, APP processing. The shedding of APP full-length occurs either by the α-secretase ADAM10/17 or by the β-secretase BACE1, generating, respectively, 83- and 99-aa-long C-terminal fragments of APP (*APP-C83* and *APP-C99*). The further processing of APP-C83 and APP-C99 by γ-secretase led to the production of the peptides p3 and Aβ, respectively, the latter of which are directly implicated in the pathological cascade of events causing Alzheimer's disease. *B*, effects of 10 μM biometals on the processing of recombinant APP-C99 substrate (*rAPP-C99*) by purified γ-secretase. Cleavage products AICD and Aβ were detected by Western blotting analysis. The γ-secretase inhibitor DAPT (1 μM) and H_2O were, respectively, used as negative and positive controls for γ-secretase activity. *C*, Zn^{2+} and Cu^{2+} inhibit rAPP-C99 processing and Aβ/AICD production in a dose-dependent manner. Indicated concentrations of Zn^{2+} and Cu^{2+} were used in the cell-free γ-secretase assay, and the cleavage products AICD and Aβ were analyzed by Western blotting. *D*, Zn^{2+} and Cu^{2+} inhibit APP processing and Aβ production in human embryonic cells. HEK 293T transiently transfected with APP-C99-FLAG were treated for 24 h with the indicated concentrations of Zn^{2+} or Cu^{2+}. After incubation, cells were collected and analyzed by Western blotting for APP-CTFs (*left panels*). Aβ1–40 peptides secreted in the culture media were quantified by ELISA, and intracellular APP-C99 levels were estimated by densitometry (*right panels*; $n = 3$). *E*, Zn^{2+} and Cu^{2+} inhibit APP processing in neurons activated with kainic acid. Rat primary cortical neurons were co-treated for 24 h with 30 μM kainic acid at indicated concentrations of Zn^{2+} or Cu^{2+}, and intracellular APP-CTFs were analyzed as described above. Cell viability was estimated by lactate dehydrogenase (*LDH*) release. All blots are representative results of at least two independent experiments. *Error bars* represent S.D. *, $p < 0.05$; **, $p < 0.01$ *versus* untreated control groups.

C99 can be observed. Our DSS approach further revealed that Cu^{2+} does not affect the quaternary structural organization of the substrate APP-C99 (Fig. 2*B*). We next compared the Cu^{2+} inhibitory effects on APP-C99 and APP-C83, the latter of which misses the N-terminal 16 amino-acids of the Aβ region containing several metal binding residues (34). Cell-free activity

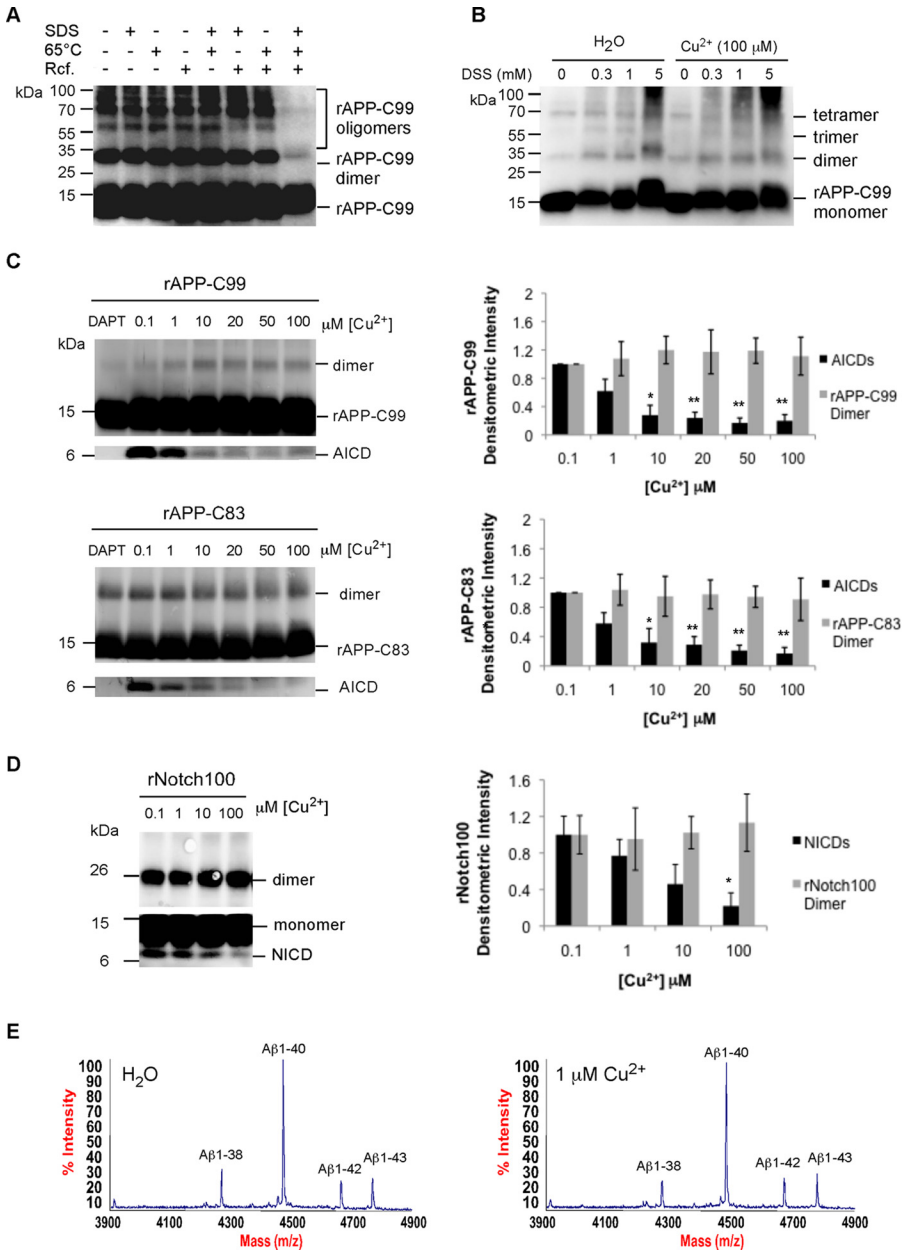

FIGURE 2. **Cu^{2+} inhibits the processing of APP and Notch by γ-secretase without affecting the substrate quaternary structure.** *A*, preparation of the rAPP-C99 substrate used in the cell-free γ-secretase activity assays. The rAPP-C99 was incubated with 0.5% SDS for 5 min at 65 °C and further centrifuged for 1 min at 11,000 × *g*. Analysis by SDS-PAGE and Western blotting reveals the clearance of the aggregated substrates. *B*, chemical cross-linking of native rAPP-C99 showing that Cu^{2+} does not affect the monomeric structure of the substrate, which is the species processed by the purified γ-secretase complex. The rAPP-C99 was incubated for 30 min at 25 °C with the indicated concentrations of the amine-reactive chemical cross-linker DSS in the presence or absence of 100 μM Cu^{2+} and analyzed by SDS-PAGE and Western blotting. *C*, Cu^{2+} inhibits the processing of both rAPP-C99 and rAPP-C83 with the same potency. Monomers and dimers of substrates and the cleavage product AICD were detected by Western blotting (*left panels*) and quantified by densitometric analysis (*right panels*; $n = 3$). *D*, Cu^{2+} inhibits the processing of a recombinant Notch-based substrate (*rNotch100*) by purified γ-secretase. Substrate monomers/dimers and cleavage product NICD were detected by Western blotting using an anti-FLAG antibody (*left panel*) and quantified by densitometric analysis (*right panel*; $n = 3$). *, $p < 0.05$; **, $p < 0.01$ *versus* 0.1 μM Cu^{2+} control groups. *Error bars* represent S.D. *E*, Cu^{2+} does not affect the specificity of rAPP-C99 cleavage and Aβ production. Cell-free γ-secretase activity assays were performed with either H_2O or 1 μM Cu^{2+} and triplicated samples were pooled and immunoprecipitated with 4G8 antibody for analysis by MALDI-MS of Aβ species. All blots are representative results of at least two independent experiments.

assays revealed (i) that the processing by γ-secretase of both APP-C99 and APP-C83 recombinant substrates was inhibited with an IC_{50} value of ~1 μM Cu^{2+}, and (ii) that Cu^{2+} did not cause substrate dimerization (Fig. 2*C*). Similarly, the processing by γ-secretase of a recombinant Notch-based substrate (rNotch100) was inhibited in a dose-dependent manner by Cu^{2+}, with an IC_{50} of ~5 μM and without causing substrate dimerization (Fig. 2*D*). We next addressed the question of whether Cu^{2+} can alter the specificity of APP processing and the profile of different Aβ-species generated in the assay. As shown in Fig. 2*E*, 1 μM Cu^{2+} (corresponding to the IC_{50} value of Cu^{2+} for the inhibition of rAPP-C99 by γ-secretase) did not affect the Aβ-profile, with Aβ40 being the major species and Aβ38, Aβ42, and Aβ43 being detected less abundantly. Altogether, our results show that the copper-mediated inhibition of γ-secretase is not substrate-specific and is not caused by sub-

strate dimerization, suggesting that it possibly occurs through a direct interaction with the protease complex.

Copper Binds Directly to the γ-Secretase Complex—The γ-secretase complex is made of the protein subunits nicastrin (NCT), the N- and C-terminal fragments of presenilin (PS1-NTF and PS1-CTF, forming the catalytic site of the enzyme), Aph1 and Pen2 (for a review, see Ref. 35). To test our hypothesis that Cu^{2+} binds directly to the γ-secretase complex, we prepared a Cu^{2+} resin (see "Materials and Methods") to complete a series of binding experiments with γ-secretase prepared from different sources. First, we found that γ-secretase solubilized from CHO cells overexpressing human PS1, Pen2-FLAG, Aph1α2-HA, and NCT-His_6 (S-20 cells; Ref. 36) bound specifically to the Cu^{2+} resin (Fig. 3*A*). We further show that γ-secretase eluted from the Cu^{2+} resin contained all subunits of the protease complex and was functionally active (Fig. 3, *A* and *B*). Next, to rule out that the strong binding of the purified γ-secretase to the copper affinity resin can be triggered by the His_6 tag fused to NCT, we performed additional affinity binding experiments by using γ-secretase solubilized from CHO cells overexpressing human PS1, Aph1α2-HA, and Pen2-FLAG but not NCT-His_6 (γ-30 cells; Ref. 37). In the presence of the endogenous, non-His_6-tagged NCT, γ-secretase was still inhibited by free Cu^{2+} (Fig. 3*C*) and still specifically bound to the copper resin (Fig. 3*D*), with the same potency and same affinity as for the purified γ-secretase harboring NCT-His_6. Next, we confirmed the binding of Cu^{2+} to the complex by using blue native gel analysis as previously reported for the metallochaperone complex Atx1 (38). We found that the migration on the blue native gel of the γ-secretase complex was clearly affected by the addition of 10 μM Cu^{2+}, as indicated by a shifted and diffuse band (Fig. 3*E*). This experiment also showed that Cu^{2+} did not inhibit γ-secretase by dissociating the protease complex, as previously observed under specific detergent conditions (37). Further supporting direct and specific copper binding to the protease complex, we found that the inhibition of γ-secretase activity caused by Cu^{2+} could be reversed by adding 10 or 100 μM free histidine but not by adding 10 or 100 μM cysteine (Fig. 3*F*). The latter further confirms that Cu^{2+} did not inhibit γ-secretase by fostering any irreversible dissociation of the protease complex.

Copper Binds to the γ-Secretase Subunits Presenilin and Nicastrin—To identify the subunit(s) within the γ-secretase complex that binds Cu^{2+} and potentially narrow-down our analysis to the identification of Cu^{2+} binding motifs within specific subunits, we completed a series of experiments in which the purified γ-secretase complex was first dissociated with the detergent Nonidet P-40 (Fig. 3*G*, *left*), and then individual subunits were analyzed for Cu^{2+} binding by affinity purification on a copper column. We found that the dissociated individual subunits PS1 and NCT (but not Aph1 and Pen2) specifically bound to the copper column (Fig. 3*G*, *middle*). Supporting this finding, we identified three potential histidine-rich copper binding sites in the γ-secretase subunits PS1-NTF (^{343}***Q***RDS***H***LGP***H***^{351}) and NCT (^{220}***H***M***H***^{222} or ^{444}***H***SGAF***H***^{449}) (Fig. 3*G*, *right*, and supplemental Fig. S2) by taking advantage of previously reported Cu^{2+} binding motifs (Refs. 39–42; listed in supplemental Fig. S2). Interestingly, PS1 is the catalytic center of the protease complex, whereas NCT has been reported to function as the substrate binding subunit of the complex (35). Targeting one or both of these subunits with copper can explain the inhibitory effects observed on APP and Notch processing.

Zinc Induces Dimerization/Oligomerization of APP-C99 That Correlates with Inhibition of Aβ Production—In contrast to Cu^{2+}, we found that Zn^{2+} did not cause any apparent conformational change in the γ-secretase complex, as monitored on blue native gel (Fig. 3*E*). However, Zn^{2+} caused a dose-dependent inhibitory effect on AICD and Aβ production that was associated with the generation of apparent APP-C99 dimers (Fig. 4*A*, *left*). The inhibition by Zn^{2+} of AICD and Aβ production (IC_{50} ~ 15 μM) was found to be as potent as the formation of the substrate dimers (EC_{50} ~ 15 μM; Fig. 4*A*, *right*), indicating that the two effects are linked. Supporting the specificity of Zn^{2+}, both phenotypes of APP-C99 dimerization and inhibition of AICD/Aβ production were prevented by the addition of the metal chelator EDTA (Fig. 4*B*). Confirming the Zn^{2+}-specific dimerization/oligomerization of APP-C99, DSS cross-linking of the native substrate incubated with 100 μM Zn^{2+} unambiguously revealed substrate dimers and higher oligomeric structures, generated in a DSS dose-dependent manner (Fig. 4*C*). Finally, analysis of the substrate by native PAGE further confirmed the formation of dimers and higher oligomers of APP-C99, under native conditions, starting at 10 μM Zn^{2+} (Fig. 4*D*).

Zinc Increases Both the Production of Aβ43 and the Aβ43:Aβ40 Ratio—We next tested by immunoprecipitation combined with mass spectrometry (IP/MS) whether Zn^{2+} can alter the specificity of APP processing and the generation of different Aβ-species. Surprisingly, Zn^{2+} was found to drastically increase the Aβ43:Aβ40 ratio in a dose-dependent manner in the range of 1–50 μM (Fig. 4*E*). No effect was observed on the Aβ42:Aβ40 ratio (Fig. 4*E*). Very similar effects were found for both $ZnSO_4$ and $ZnCl_2$ (supplemental Fig. S3), indicating that they are specific to the Zn^{2+} ion but not caused by the counterions Cl^- or SO_4^{2-}. We next investigated whether the overall effect increased or decreased Aβ43 production, and estimated by enzyme-linked immunosorbent assays (ELISA) the concentrations of Aβ43 and Aβ40 peptides generated in our cell-free γ-secretase assays in the presence of increasing concentrations of Zn^{2+}. We found that 20 μM Zn^{2+} caused a ~50% increase in the production of the Aβ43 peptides, associated with a ~50% reduction in Aβ40 production when compared with the control reaction without Zn^{2+} (Fig. 4*F*). Altogether, these results not only confirm the fact that Zn^{2+} increases the Aβ43:Aβ40 ratio (by 2.5-fold and 5-fold at Zn^{2+} concentrations of 20 and 50 μM, respectively), but they also reveal that Zn^{2+} is as a newly identified Aβ43 raising factor. This is important, as Aβ43 has previously been reported to be a pathological marker of AD (43, 44), suggesting the possibility that increased Aβ43 production can initiate or participate to the pathological processes causing AD.

The Zinc-dependent Effects on APP-C99 Dimerization and Inhibition of AICD/Aβ Production Require the 16 N-terminal Residues of the Aβ Domain—Zn^{2+} was found in Aβ plaques and was previously reported to target Aβ peptides by binding with high affinity the histidine residues His-6, His-13, and His-14

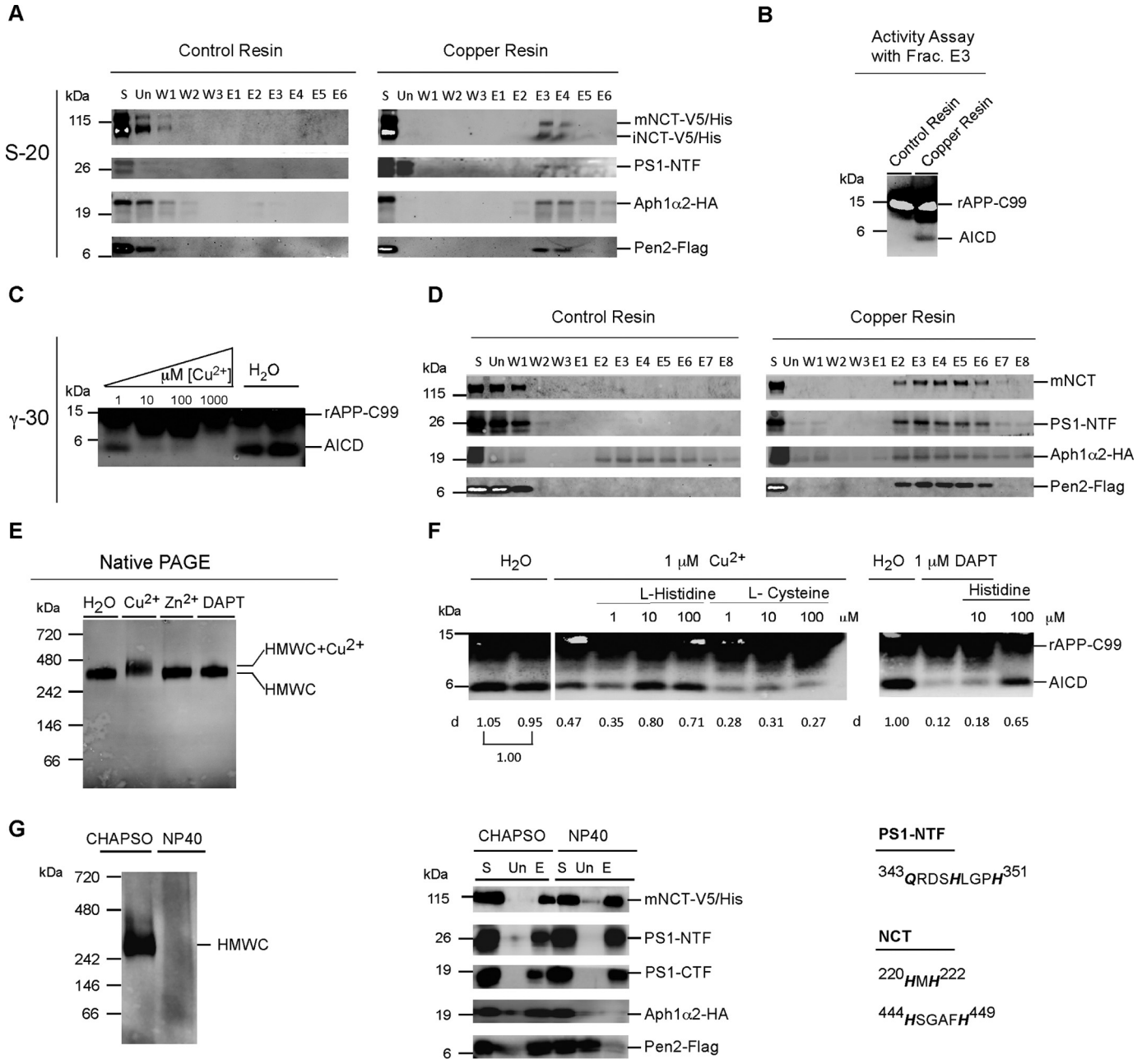

FIGURE 3. **Cu^{2+} binds directly to the γ-secretase complex.** *A*, purification of γ-secretase using a Cu^{2+} affinity column. First, membranes from CHO cells overexpressing γ-secretase (*S-20*) were solubilized in a buffer containing 0.25% CHAPSO, and the solubilized material (*S*) was loaded on the Cu^{2+} affinity column. Next, the unbound fraction (*Un*) was collected, the resin was subjected to three successive washes (*W1*, *W2*, *W3*), and the bound proteins were eluted with 20 mM imidazole in 6 equal fractions (*E1* to *E6*). Finally, all collected fractions were analyzed by Western blotting for all γ-secretase subunits. *B*, the elution fractions E3 from both the control column (resin without Cu^{2+}) and the Cu^{2+} affinity column were tested for γ-secretase activity with the substrate rAPP-C99, and the cleavage product AICD was detected by Western blotting analysis using the anti-FLAG antibody M2. *C* and *D*, the inhibition of γ-secretase by Cu^{2+} and the specific binding of the protease complex to the copper affinity column are independent of the His tag on NCT-His_6. *C*, Cu^{2+} inhibits rAPP-C99 processing by γ-secretase-containing endogenous NCT (*γ-30* cells). *D*, the affinity purification of γ-secretase solubilized from γ-30 membranes was performed as described above for the S20 cells, except that the bound proteins were eluted in eight equal fractions (*E1* to *E8*). *E*, Cu^{2+} binds the native γ-secretase complex. Purified γ-secretase solubilized in a buffer containing 0.1% CHAPSO was preincubated at 37 °C for 2 h with 10 μM Cu^{2+}, 10 μM Zn^{2+}, 1 μM DAPT, or H_2O. The samples were analyzed by blue native PAGE on a 4–16% gel, and the migration of the high molecular weight protease complex (*HMWC*) was analyzed by Western blotting using an anti-NCT antibody (NCT164). Note the modified migration of the γ-secretase complex in the presence of Cu^{2+}. *F*, the Cu^{2+}-dependent inhibition of γ-secretase is specifically reversed by the metal chelating agent histidine. Purified γ-secretase was incubated at 37 °C for 4 h with 1 μM Cu^{2+} or 1 μM DAPT together with the indicated concentrations of L-histidine or L-cysteine. The reactions were stopped, and the resulting cleavage product AICD was analyzed by Western blotting using the anti-FLAG antibody M2 and quantified by densitometric analysis. *G*, Cu^{2+} binds to the γ-secretase subunits PS1 and NCT. Purified γ-secretase was first solubilized in 1% CHAPSO, which preserves the entity of the complex, or in 1% Nonidet P-40, which triggers the physical dissociation of individual subunits (*left*). Next, the preparations were incubated overnight with the Cu^{2+} affinity resin and subjected to three successive washes, and the bound proteins were eluted with 20 mM imidazole (*middle*). Three potential copper binding sites were identified in the γ-secretase subunits PS1 and NCT (*right*). All blots are representative results of at least two independent experiments.

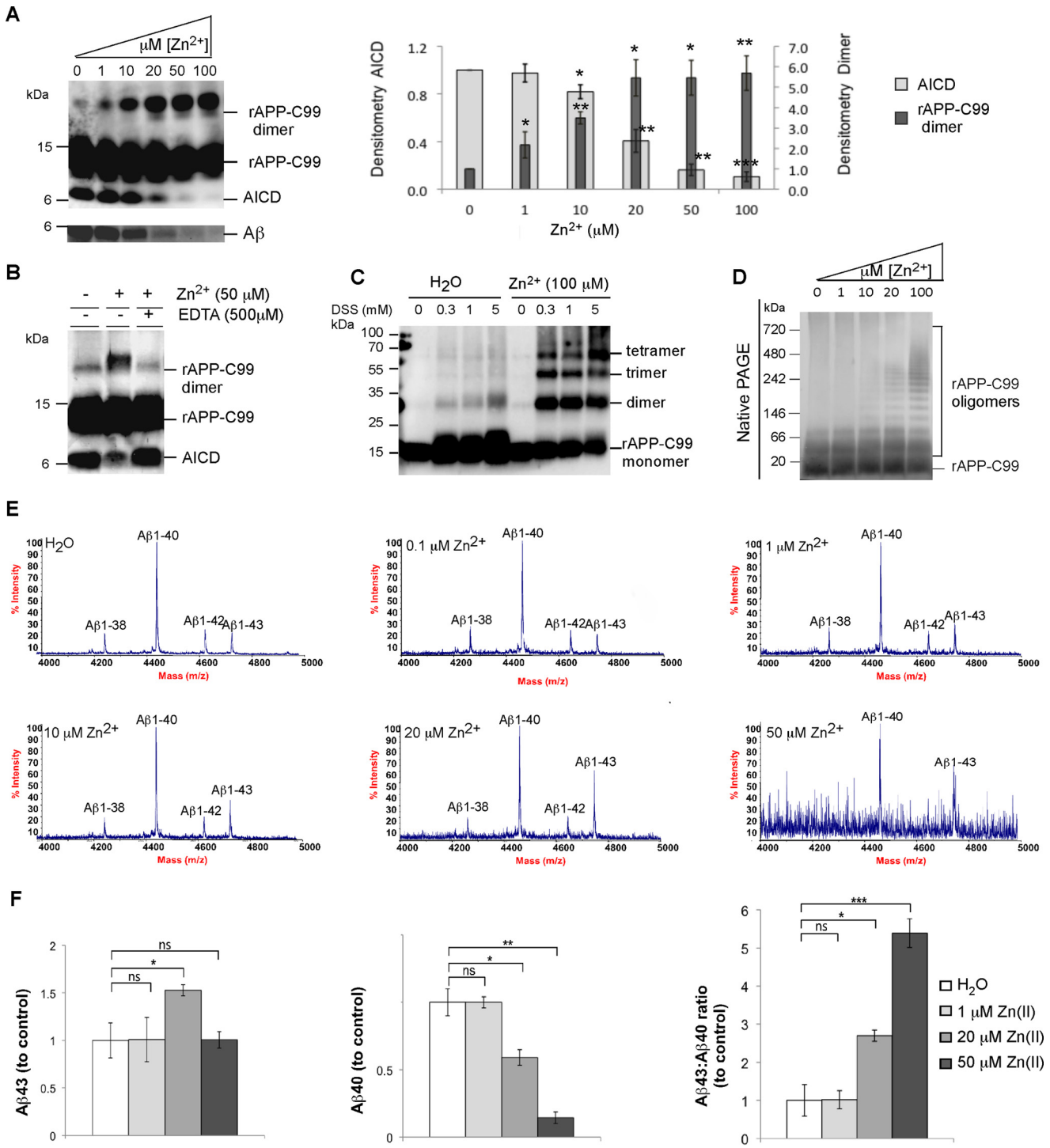

FIGURE 4. **Zn^{2+} raises the Aβ43:Aβ40 ratio and inhibits the processing of APP-C99 by substrate dimerization/oligomerization.** *A*, Zn^{2+} triggers a dose-dependent dimerization of rAPP-C99 that correlates with the inhibition of AICD and Aβ production. γ-Secretase activity assays were performed in the presence of the indicated concentrations (μM) of $ZnCl_2$. The monomeric and dimeric rAPP-C99 as well as the resulting AICD and Aβ cleavage products were resolved by SDS-PAGE and detected with antibodies targeting APP or Aβ (*left*). The relative levels of AICD and rAPP-C99 dimers were quantified by densitometry (right; $n = 3$). *, $p < 0.05$; **, $p < 0.01$; ***, $p < 0.001$ *versus* untreated control groups. *Error bars* represent S.D. *B*, the metal chelator EDTA prevents the Zn^{2+}-dependent dimerization of rAPP-C99 and its processing by γ-secretase. *C*, chemical cross-linking of native rAPP-C99 shows the formation of substrate dimers and higher oligomers. The substrate rAPP-C99 was incubated for 30 min at 25 °C with the indicated concentrations of the amine-reactive chemical cross-linker DSS in the presence or in the absence of 100 μM Cu^{2+} and analyzed by SDS-PAGE and Western blotting. *D*, native PAGE (4–16%) analysis by Western blotting of rAPP-C99 incubated with increased concentrations of Zn^{2+} shows the formation in a dose-dependent manner of substrate dimers and higher oligomers under native conditions after incubation for 2 h at 37 °C in the same buffer as that used for the γ-secretase activity assay. *E*, Zn^{2+} drastically modifies the Aβ profile by raising the Aβ43:Aβ40 ratio. The γ-secretase activity assays were conducted in the presence of Zn^{2+} at indicated concentrations or H_2O (control), and Aβ peptides were immunoprecipitated with the 4G8 antibody and analyzed by MALDI-MS. *F*, Zn^{2+} raised the production of Aβ43 and the Aβ43:Aβ40 ratio. The Aβ40 and Aβ43 peptides generated as in *E* by purified γ-secretase were quantified by ELISA (*left* and *middle*; $n = 3$), and the values were used to estimate Aβ43:Aβ40 ratios (*right*; $n = 3$). *, $p < 0.05$; **, $p < 0.01$; ***, $p < 0.001$ *versus* water-treated control groups. *ns*, non significant. *Error bars* represent S.D. All blots are representative results of at least two independent experiments.

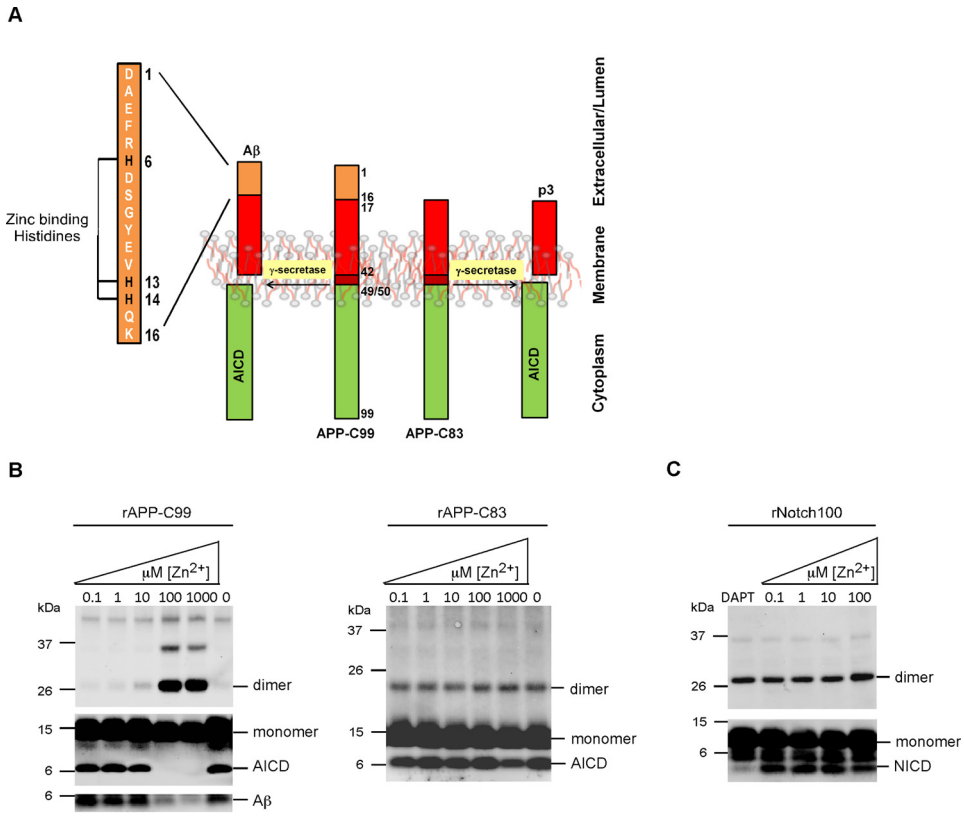

FIGURE 5. **Zn^{2+} specifically inhibits the processing of APP-C99 without affecting the cleavage of APP-C83 or a Notch-based substrate.** *A*, schematic representation of APP-C99 and APP-C83 substrates processed by γ-secretase, with highlights on the known Zn^{2+} binding residues His-6, His-13, and His-14 that are present on APP-C99 but not on APP-C83. *B* and *C*, Zn^{2+} triggers substrate dimerization and γ-secretase cleavage inhibition for rAPP-C99 but not for rAPP-C83 or the Notch-based substrate rNotch100. Activity assays performed with purified γ-secretase were carried out at the indicated Zn^{2+} concentrations, and the full-length substrates and cleavage products were resolved by SDS-PAGE (4–12% gel) and further analyzed by Western blotting with an anti-FLAG antibody (M2; to detect FLAG-tagged full-length rAPP-C99, rAPP-C83, and rNotch100 and FLAG-tagged cleavage products AICD and NICD) and an anti-Aβ antibody (6E10; to detect Aβ). All blots are representative results of at least two independent experiments.

(Fig. 5*A*) (10). Substrates lacking those residues were used to further test the implication of the histidine-rich motif in the Zn^{2+}-dependent effects on APP-C99 processing by γ-secretase (Fig. 5*B*). In contrast to the effects observed on APP-C99, Zn^{2+} did not induce the formation of APP-C83 dimers and did not inhibit the processing of this substrate by γ-secretase, even at concentrations as high as 100 μM (Fig. 5*B*). Similarly, no effects were observed on the Notch-based substrate at Zn^{2+} concentrations up to 100 μM (Fig. 5*C*). Taken together, we demonstrate that the N-terminal 16 aa residues of the Aβ-domain are required for the Zn^{2+}-dependent effects on APP-C99 dimerization and inhibition of AICD/Aβ production.

The Histidines of the Aβ Domain Are Implicated in the Zn^{2+}-dependent Dimerization of APP-C99 and Inhibition of AICD/Aβ Production—To identify the Zn^{2+} binding sites controlling APP-C99 dimerization/oligomerization, we generated and purified the recombinant APP-C99 substrates harboring single, double, and triple histidine to alanine mutations at the positions His-6, His-13, and His-14 (Fig. 6*A*, *left* and *middle*), all of which have previously been reported to be implicated in Aβ oligomerization (10). In the absence of exogenously added Zn^{2+}, all substrates were equally cleaved by γ-secretase (Fig. 6*A*, *right*), and the mass spectrometric analysis of the Aβ species showed that the processing of all histidine to alanine mutants is very similar to that observed for the wild type (WT) substrate, with the main Aβ species being Aβ40 and minor peaks for Aβ38, Aβ42, and Aβ43 (Fig. 6*B*). In the presence of 100 μM Zn^{2+}, the single mutants H6A, H13A, and H14A did not prevent substrate dimerization and γ-secretase inhibition (Fig. 6*C*). In contrast, the double mutants H6A/H13A and H6A/H14A showed reduced dimerization of APP-C99, associated with increased γ-secretase substrate processing. Strikingly, the double mutant H13A/H14A and the triple mutant H6A/H13A/H14A showed an almost complete resistance to Zn^{2+}-induced dimerization of APP-C99, associated with a drastic increase in substrate cleavage and AICD/Aβ production (Fig. 6*C*). Together, our findings suggest that Zn^{2+} predominantly binds to APP-C99 and induces substrate dimerization by coordination of the His-13 and His-14 residues to the metal (Fig. 6*D*, *left*). They further suggest that Zn^{2+} can also dimerize APP-C99 by coordinating the His-6 residue together with one of the residues His-13 or His-14 (Fig. 6*D*, *right*).

The Zn^{2+}-dependent Increase of the Aβ43:Aβ40 Ratio Is Independent of Zn^{2+} Coordination to Residues His-6, His-13, and His-14—We next tested whether the increased Aβ43:Aβ40 ratio observed with the WT APP-C99 is somehow linked to the Zn^{2+} coordination to the residues His-6, His-13, and His-14. Thus, we performed cell-free γ-secretase activity assays with both the WT and the triple mutant H6A/H13A/H14A APP-C99 substrates at Zn^{2+} concentrations ranging from 0 to 100

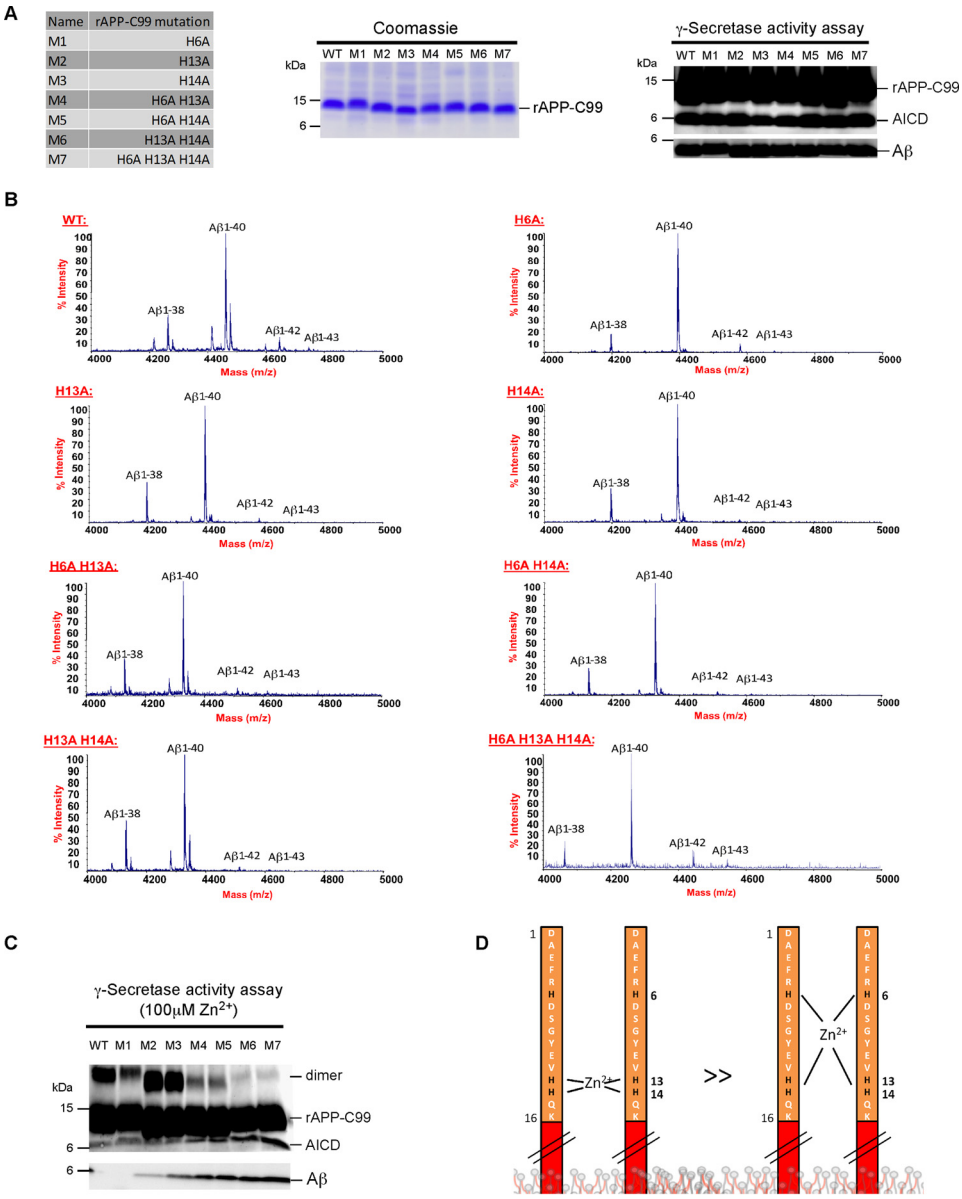

FIGURE 6. **Zn^{2+} triggers APP-C99 dimerization and inhibition of its cleavage by γ-secretase mainly through binding to the substrate at positions His-13 and His-14.** *A*, cell-free γ-secretase activity assays performed in the absence of Zn^{2+} with WT and mutated APP-C99 substrates. The single, double, and triple histidine to alanine rAPP-C99 mutants at positions 6, 13, and 14 (listed in the *left panel*) were purified, and BCA-normalized protein substrates were analyzed by SDS-PAGE on a Coomassie-stained 4–12% gel (*middle*) and used for γ-secretase activity assays (*right*). The full-length substrates as well as the cleavage products were resolved by SDS-PAGE on a 4–12% gel and analyzed by Western blotting with an anti-APP antibody (CT15; to detect APP-C99 and AICD) and the Aβ specific antibody 4G8 (*right*). *B*, IP/MS analyses of Aβ peptides generated in cell-free γ-secretase activity assays were performed in the absence of Zn^{2+} with WT and mutated rAPP-C99 substrates. *C*, cell-free γ-secretase activity assays performed in the presence of 100 μM Zn^{2+} with WT and mutated APP-C99 substrates. Full-length substrates and cleavage products were detected as described above. *D*, schematic representation of APP-C99 dimerization through Zn^{2+} coordination mainly to residues His-13 and His-14 (*left*) and to a lesser extent to the histidine pairs His-6/His-13 or His-/His-14 (*right*). All blots are representative results of at least two independent experiments.

μM. Notably, the APP-C99 triple mutant M7 (as well as the substrates M2 to M6) shows a different apparent mobility when compared with the WT and M1 variants (Figs. 7*A* and 6*C*), which can be attributed to different charges and/or conformational changes. Consistent with the above-described results, Zn^{2+} concentrations >10 μM caused the dimerization of the WT APP-C99 and inhibited AICD/Aβ production (Fig. 7*A*). In sharp contrast, histidine-to-alanine substitutions in the triple mutant APP-C99 substrate did prevent those effects (Fig. 7*A*). Very similar results were obtained for the APP-C99 H13A/H14A double mutant, confirming that histidine residues His-13 and His-14 are the main residues involved in APP-C99 dimerization (supplemental Fig. S4). At high concentrations (100 μM), Zn^{2+} also initiated some dimerization of the double/triple His-to-Ala APP-C99 substrate mutants and AICD inhibition but with a much lower affinity when compared with the WT substrate (apparent IC_{50} values for AICD production are >100 μM for both mutants compared with 15 μM for the WT substrate; Fig. 7*A* and supplemental Fig. S4). It suggests that in the absence of the His-13/His-14 residues, Zn^{2+} can trigger substrate dimerization by binding to yet unidentified amino acid residues. Further confirming that the histidine residues

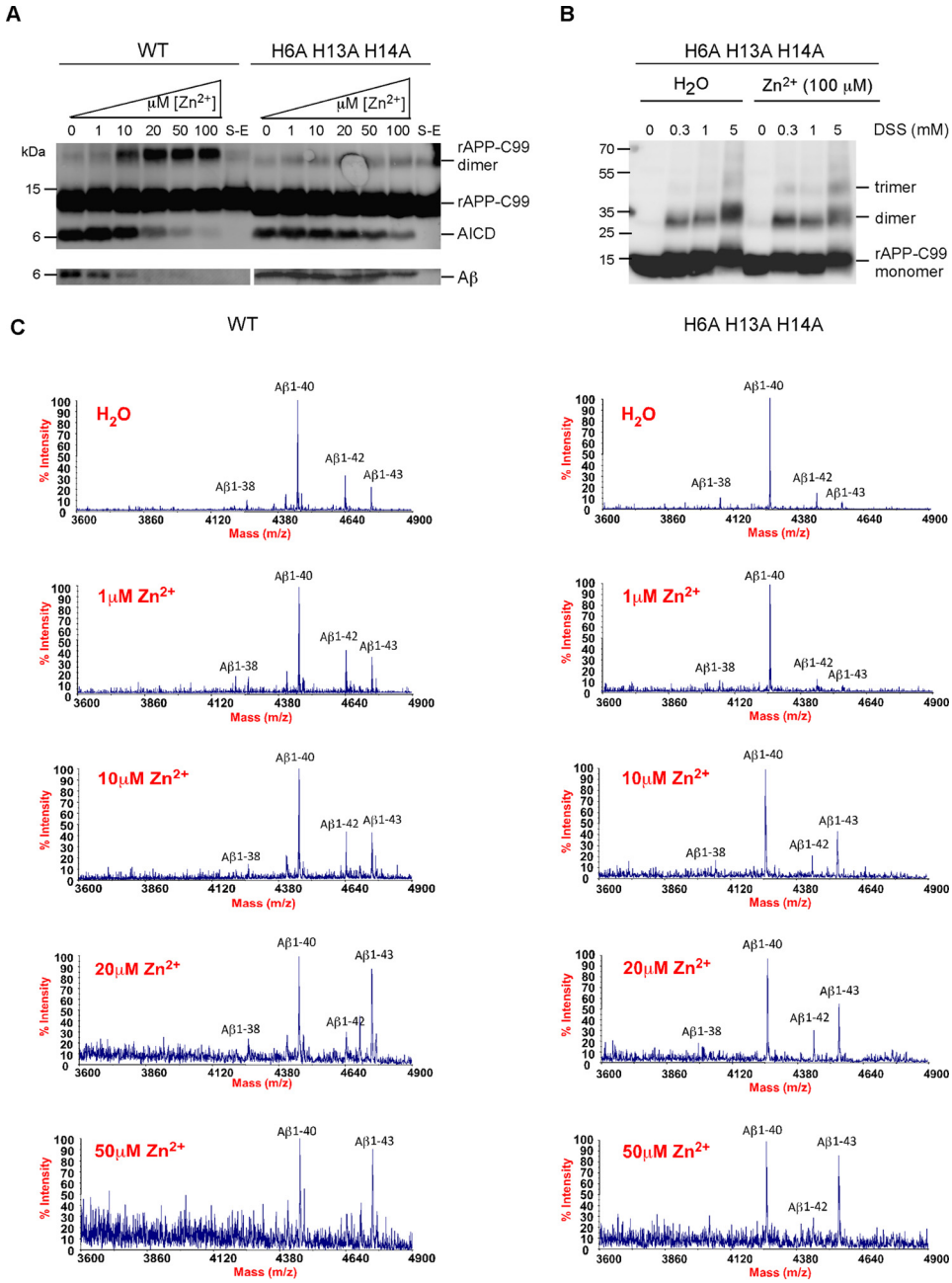

FIGURE 7. **The residues His-6, His-13, and His-14 causing APP-C99 dimerization/oligomerization by Zn^{2+} are not implicated in the Zn^{2+}-dependent increase of the Aβ43:Aβ40 ratio.** *A*, cell-free γ-secretase activity assays were performed with the WT or the H6A/H13A/H14A triple-mutated APP-C99 substrates in the presence of 0–100 μM Zn^{2+}. Monomeric and dimeric APP-C99 substrates and the AICD cleavage product were detected by SDS-PAGE (4–12%) and Western blotting with the antibody CT15. Aβ peptides were detected with the antibody 4G8. *S-E*, control reactions with substrate (*S*) but minus the enzyme (−*E*). *B*, chemical cross-linking of the native H6A/H13A/H14A triple-mutated APP-C99 substrate showing that Zn^{2+} does not affect the quaternary structure of this substrate. rAPP-C99 was preincubated in the presence or in the absence of 100 μM Zn^{2+} at 37 °C and then incubated for 30 min at 25 °C with the indicated concentrations of the amine-reactive chemical cross-linker DSS and analyzed by SDS-PAGE and Western blotting. *C*, IP/MS analyses of Aβ peptides generated in γ-secretase activity assays performed with the WT and the triple-mutated H6A/H13A/H14A APP-C99 substrates in the presence of 0–50 μM Zn^{2+}. All blots are representative results of at least two independent experiments.

His-13 and His-14 are the main residues involved in APP-C99 dimerization, DSS cross-linking of the native triple mutant APP-C99 incubated with 100 μM Zn^{2+} did not trigger substrate dimerization/oligomerization (Fig. 7*B*). Next, we compared the mass spectrometric Aβ profiles of both APP-C99 WT and triple mutant H6A/H13A/H14A at different Zn^{2+} concentrations (Fig. 7*C*). A drastic Zn^{2+}-dependent increase of the Aβ43:Aβ40 ratio was found in both WT and triple mutant APP-C99 substrates, demonstrating that the phenotype of increased Aβ43:Aβ40 ratio with increased Zn^{2+} was independent of the Zn^{2+} binding to the histidine residues His-6/-13/-14.

The Lysine Residue Lys-28 of the Aβ Domain Is Implicated in the Zn^{2+}-dependent Increased Aβ43:Aβ40 Ratio—Zn^{2+} has recently been reported to cause major structural changes in the N-terminal domain of Aβ by coordination to the residue Lys-28 and by consequently breaking the salt bridge between the side chains of the residues Asp-23 and Lys-28 (45). Interestingly, the residue Lys-28 is located directly at the extracellular border of

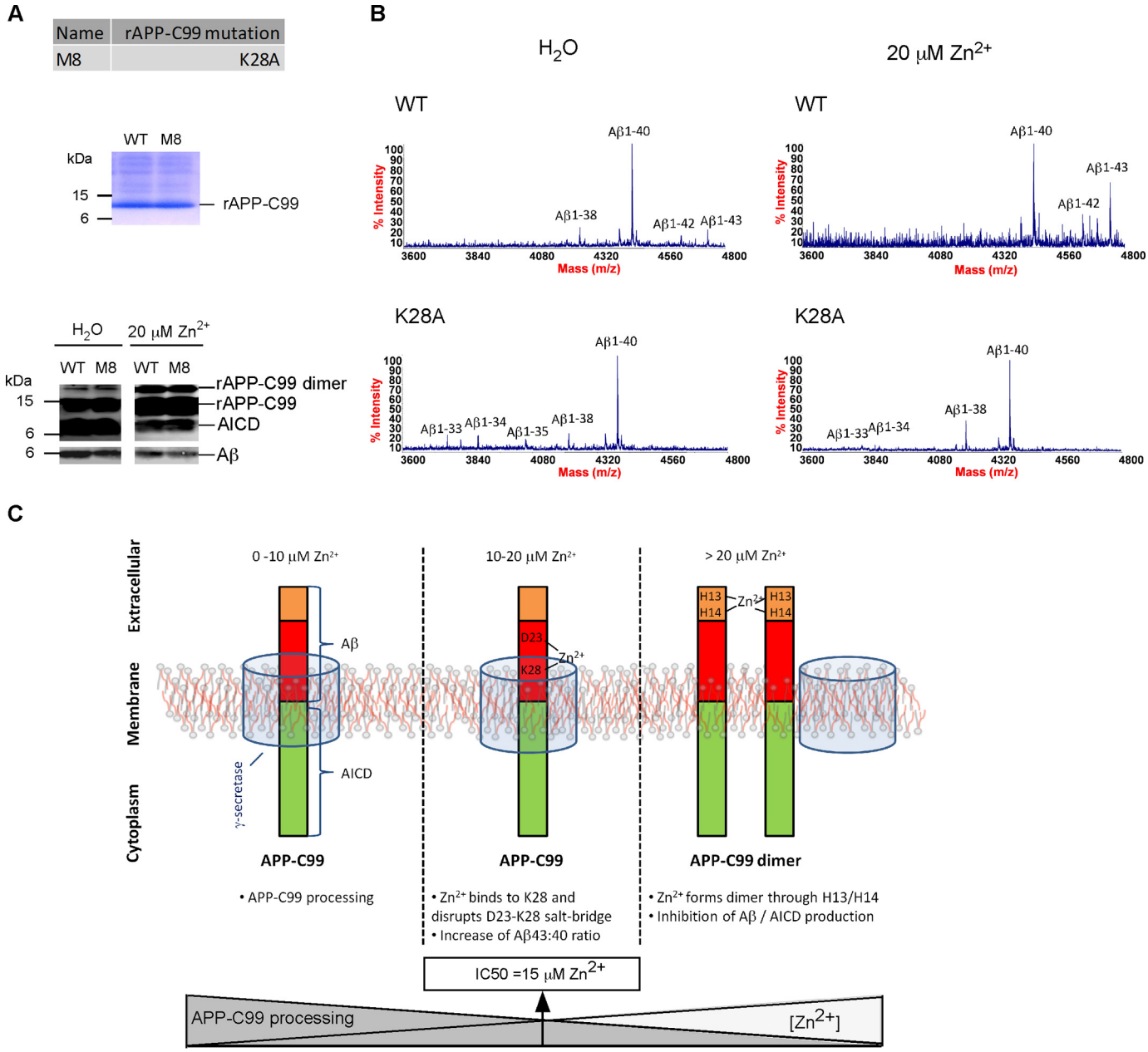

FIGURE 8. **The known Zn^{2+} binding residue Lys-28 of APP-C99 regulates the production of Aβ43 and Aβ42.** *A*, the recombinant APP-C99 WT and mutated K28A substrates (*M8*, *upper panel*) were analyzed by SDS-PAGE on a Coomassie-stained 4–12% gel (*middle panel*) and used in γ-secretase activity assays performed in the presence or in the absence of 20 μM Zn^{2+} (*bottom panel*). Substrates and cleavage products were analyzed by Western blotting with an anti-APP antibody (CT15; to detect rAPP-C99 and AICD) and the Aβ-specific antibody 4G8. *B*, Aβ peptides were further analyzed by IP/MS. *C*, putative model for the Zn^{2+}-dependent modulation of APP-C99 processing by γ-secretase through binding to the substrate at positions Lys-28 and His-13/His-14. In this model Zn^{2+} concentrations around the IC_{50} value for γ-secretase inhibition of APP-C99 processing (~15 μM) triggered increased Aβ43 production and increased Aβ43:Aβ40 ratio, presumably through a modified positioning of the substrate TMD in the lipid bilayer caused by the binding of Zn^{2+} to lysine residue Lys-28. At higher concentrations zinc coordination mainly to the histidine pair His-13/His-14 initiated substrate dimerization/oligomerization, which prevents the processing of APP-C99 by γ-secretase and inhibits Aβ/AICD production. All blots are representative results of at least two independent experiments.

the membrane, from where it can possibly regulate the position/orientation of the APP-C99 transmembrane domain (TMD) in the membrane bilayer relative to the γ-secretase active site (46, 47). Given these observations, we hypothesized that Zn^{2+} coordination to the residue Lys-28 can affect the specificity of Aβ production by causing structural changes in the N-terminal Aβ-domain of APP-C99. To test whether Lys-28 can contribute to the increased Aβ43:Aβ40 ratio, we generated and purified the APP-C99 WT and mutant K28A substrates that we further used in our cell-free γ-secretase assay. In the absence of exogenously added Zn^{2+}, both substrates where readily cleaved by γ-secretase (Fig. 8*A*). Remarkably, the mass spectrometric analysis of the Aβ species showed that the processing of the APP-C99 mutant K28A in the absence of zinc is characterized by the complete disappearance of longer Aβ species including Aβ43 and Aβ42, the latter of which was associated with the appearance of shorter Aβ species including Aβ34 and Aβ33 (Fig. 8*B*). The presence of 20 μM Zn^{2+} did not modulate Aβ production toward longer species (Fig. 8*B*). Together, these results confirm that residue Lys-28

indeed regulates the specificity of Aβ production and further suggest that Zn^{2+} binding to Lys-28 can potentially contribute to the phenotypes of increased Aβ43 production and increased Aβ43:Aβ40 ratio, observed in WT APP-C99.

Discussion

Copper and zinc have both been associated with neurodegeneration and AD (48). Because the various mechanisms proposed to explain the link between alteration of copper and zinc homeostasis and the pathological processes causing AD remain largely controversial, we investigated whether those biometals can interfere with the production of the Aβ peptides known to play a central role in this brain disorder. More specifically, we studied whether free copper and zinc can directly interfere with one of the enzymatic players of Aβ production, namely the γ-secretase enzyme and the substrate APP-C99. Our findings demonstrate that Cu^{2+} is a direct γ-secretase inhibitor affecting APP processing and AICD/Aβ production in cell-free and cell-based systems, with IC_{50} values of ~1 μM and ~70 μM, respectively. As expected from an inhibitor targeting the enzyme (*versus* the substrate), Cu^{2+} also affected the processing of the Notch receptor. One can thus suspect that the processing of other known γ-secretase substrates is altered by this metal. In contrast to Cu^{2+}, we also demonstrate that Zn^{2+} directly targets the substrate APP-C99 and inhibits its processing in cell-free and cell-based systems, with IC_{50} values of ~15 μM and ~20 μM, respectively. We also found that Zn^{2+} is an Aβ43-raising biometal that increases the Aβ43:Aβ40 ratio. In comparison, human brain concentrations of bioavailable Cu^{2+} and Zn^{2+} were reported to be 70 μM and 350 μM, respectively (4), making our findings potentially important physiologically.

Copper and AD—The copper content in a healthy human adult brain represents 7–10% of total body copper and is particularly enriched in the hippocampus and substantia nigra (49). A multitude of studies has associated aging and AD with elevated brain copper levels and abnormal brain copper homeostasis, resulting in the "metal hypothesis of AD." First, copper levels have been estimated in different studies to elevate with aging and to be increased in AD brains (50, 51), reaching concentrations up to 390 μM in AD brain as compared with normal age-matched samples (70 μM) (4). Copper dyshomeostasis can either (i) facilitate the generation of free radicals and cause oxidative stress-induced damage to neurons (52), (ii) induce Aβ aggregation and senile plaque formation (52), (iii) alter synaptic functions by interfering with the glutamatergic system (53, 54), or (iv) induce aggregation of the protein Tau (55, 56), all of which recapitulate what is observed in AD. Supporting the metal hypothesis, elevated free copper in the blood of AD patients has also been reported to negatively correlate with cognition and even predict the rate of loss of cognition (57).

Next, remarkably high concentrations of copper (400 μM) have been reported in senile plaques isolated from AD subjects (4), and a consensus has emerged that μM concentrations of copper released from neuronal synapses are sufficient to induce Aβ aggregation (58, 59).

Interestingly, in the last decade, a growing list of physiological functions has been suggested for γ-secretase in developing and adult neurons that are modulated through APP and Notch sequential processing pathways and its residual cleavage products. This list includes essential roles in synaptic plasticity, learning, and memory (60–67). Very strong evidence supporting an implication of γ-secretase in neuronal functions came from the conditional presenilin KO mouse, which recapitulated some neuronal phenotypes characteristics of AD (62). Clinical trials with γ-secretase inhibitors have also led to cognitive defects when compare with the placebo group (68).

Because we demonstrate in this study that copper targets γ-secretase and modulates the processing of both APP and Notch substrate, but also because of the changes in copper contents observed in AD brains, one can hypothesize that copper dyshomeostasis or exposure to high copper concentrations in adult life can impact the neuronal functions of γ-secretase and other synaptic proteins, impair learning and memory, and potentially participate to neuro-pathophysiological processes that cause AD. This hypothesis is supported by Wilson disease (WD), which is the paradigmatic disease of copper accumulation and intoxication. WD is an autosomal recessive genetic disorder caused by mutations in the copper transporter ATP7B that trigger a defect in copper excretion and consequently an increase in copper levels in the general circulation, which in turn leads to copper overloads in the liver and in the brain (69). Interestingly, genetic variants in ATP7B have also been associated with a significant increase in AD risk (reviewed in Ref. 70).

Together, current clinical and experimental evidence suggests that copper dyshomeostasis in WD and AD share some pathogenic mechanisms. It also suggests that clinical copper chelators may be beneficial in both the prevention and the treatment of AD, an hypothesis that has largely motivated the development of the so-called metal protein attenuating compounds (MPACs) and their tests in human clinical trials (reviewed in Refs. 71–73). Among those compounds, 5-chloro-7-iodo-quinolin-8-ol (clioquinol) prevented cognitive deterioration and lowered plasma Aβ42 levels of 36 weeks in a phase 2 clinical trial of 32 patients (74). Although these data sounded promising, difficulties with the large scale manufacturing of this compound have apparently prevented further clinical studies. Second generation 8-hydroxyquinoline metal protein attenuating compounds have then been generated, based on the chemical scaffold of clioquinol. These compounds include PBT2, which lowered cerebrospinal fluid levels of Aβ1–42 and improved cognitive performance in a phase 2a clinical trial of 78 patients with early AD over a 12-week treatment period (21, 75). Unfortunately, PBT2 did not show favorable clinical outcomes in a following phase 2b clinical trial.[4] Based on these overall encouraging results, low-copper diets have been proposed as preventive strategies for AD (76).

Zinc and AD—The physiological serum concentration of Zn^{2+} is around 10 μM (77), whereas the free Zn^{2+} in the synaptic cleft reached concentrations of ~300 μM after neurotransmission and release from synaptic vesicles (34). ZnT3, the transporter of Zn^{2+} into those vesicles, is mainly expressed

[4] Prana Biotechnology announced preliminary results of the Phase 2 IMAGINE trial of PBT2 in Alzheimer's disease" (March 31, 2014). Prana Biotechnology, Melbourne, Australia.

in brain areas where AD pathology occurs, including the hippocampus, cortex, and olfactory bulb (78). Further supporting a molecular link between zinc homeostasis and AD, mice depleted in ZnT3 display Alzheimer's disease-like cognitive phenotypes, including reduced learning and memory performances (22). The molecular link between Zn^{2+} and AD is further suggested by a Zn^{2+}-dependent modulation of (i) the levels of toxic Aβ species in the human cerebrospinal fluid (79) and (ii) Aβ oligomerization and senile plaque formation (4, 5).

In our study we first observed a Zn^{2+}-dependent specific and direct inhibition of the processing of the substrate APP-C99 by purified γ-secretase, with an IC_{50} value of ~ 15 μM (Fig. 4). This result was consistent with a previous study showing (without providing a molecular explanation) that this biometal can inhibit the γ-secretase-dependent processing of APP-C99 (80). Interestingly, we found that Zn^{2+} was able to promote both dimerization and oligomerization of the substrate APP-C99 and that those structural changes perfectly correlated with the inhibition of substrate processing (Fig. 4). Interestingly, homodimerization of APP-C99 via cross-linking at engineered cysteine residues also inhibited substrate processing (81). Next, we found that the Zn^{2+} binding histidine residues His-13 and His-14 are the main residues causing APP-C99 dimerization/oligomerization (Figs. 6 and 7). Importantly, a detailed IP/MS analysis of the Aβ species revealed that Zn^{2+} was able to specifically and drastically raise the Aβ43:Aβ40 ratio (Figs. 4 and 6). Quantifications by ELISA of Aβ43 further revealed that Zn^{2+} was able to raise the production of Aβ43 (Fig. 4). To the best of our knowledge this is the first report showing experimental conditions that cause the increase of both Aβ43 production and Aβ43:Aβ40 ratio. This is important because special attention has recently been given to the Aβ43 species and its potential neurotoxicity and role in the pathogenesis of AD, mainly because Aβ43 has been found in the senile plaques of human AD brains (43).

At the molecular level the residues His-13 and His-14 involved in the zinc-dependent dimerization/oligomerization of APP-C99 are not implicated in the increased Aβ43:Aβ40 ratio (Fig. 7), suggesting that the two zinc-dependent phenotypes, namely substrate dimerization/oligomerization and increased Aβ43 production/Aβ43:Aβ40 ratio, are not mechanistically linked. The production of Aβ43 and Aβ42 is controlled by the positively charged lysine residue Lys-28 of APP-C99 (Fig. 8 and Ref. 45), which guides the positioning of the substrate TMD in the lipid bilayer (45, 46). Interestingly, Lys-28 is a known Zn^{2+} binding site (82), raising the possibility that zinc coordination to this residue is responsible for the Zn^{2+}-specific Aβ43:Aβ40 increase. Yet, because Aβ43 is known to be a direct precursor of Aβ40 (83), the increased Aβ43 production suggests that Zn^{2+} blocks the sequential processing of APP-C99 at the Aβ43 position. In agreement with that, we found that Zn^{2+} was not able to affect the ϵ-cleavage of APP-C99 and the production of AICD50–99 and AICD49–99 (supplemental Fig. S5).

Altogether, our findings support a model depicted in Fig. 8*C* in which Zn^{2+} concentrations around the IC_{50} value for γ-secretase inhibition of APP processing (~15 μM) led to increased Aβ43 production and Aβ43:Aβ40 ratio through a molecular mechanism that does not involve substrate dimerization/oligomerization but possibly a modified positioning of the TMD in the lipid bilayer caused by the binding of Zn^{2+} to the lysine residue Lys-28. At higher concentrations, zinc coordination mainly to the histidine residues His-13 and His-14 triggers substrate dimerization/oligomerization, the latter of which prevents the processing of APP-C99 by γ-secretase and Aβ/AICD production.

Conclusions—We show here that zinc and copper differentially modulate γ-secretase processing of APP-CTFs and the production of the Alzheimer's Aβ peptides. By binding copper binding sites on γ-secretase, Cu^{2+} inhibits the processing of all substrates tested, including APP-C99, APP-C83, and Notch. In contrast, Zn^{2+} specifically targets APP-C99 and causes two independent phenotypes: increased Aβ43 production/Aβ43:Aβ40 ratio and substrate dimerization/oligomerization inhibiting Aβ/AICD production. Specifically, reducing Aβ production by targeting the γ-secretase cleavage of APP-C99 without affecting the physiological processing of APP-C83 and other substrates is a potential strategy for safely treating AD. Tested approaches include APP-C99 substrate targeting small molecule inhibitors (84) or APP-C99 substrate neutralizing specific monoclonal antibodies (85). Our data also suggest that zinc provides another alternative to specifically reduce Aβ production but also that any substrate targeting therapeutic strategy should carefully exclude potential off-target effects caused by modified APP-C99 processing leading, for example, to increased Aβ43 production and/or increased Aβ43:Aβ40 ratio.

Materials and Methods

Reagents—Chemicals were bought from commercial sources: $CuCl_2{\cdot}2H_2O$, $CaCl_2{\cdot}2H_2O$, $ZnCl_2$, $CdCl_2{\cdot}2.5H_2O$, $NiCl_2{\cdot}6H_2O$, $CoCl_2{\cdot}6H_2O$, $AlCl_3$, LiCl, L-cysteine, L-histidine, and DAPT (*N*-[*N*-(3,5-difluorophenylacetyl)-L-alanyl-]-(*S*)-phenylglycine-*t*-butyl ester) were purchased from Sigma. $ZnSO_4{\cdot}7H_2O$, $MgCl_2{\cdot}6H_2O$, and $MnC_4H_6O_4{\cdot}2H_2O$ was from Applichem (Darmstadt, Germany). Protease inhibitors were obtained from Roche Applied Science. LDH cytotoxicity assay and DSS were obtained from Pierce. The ELISA kit for human Aβ40 was purchased from Invitrogen, and the ELISA kit for Aβ1–43 was from IBL.

Cell Lines and Cell Cultures—HEK 293T cells transiently transfected with APP-C99-FLAG (86) were maintained in DMEM with 10% FBS. Rat primary cortical neurons were prepared and cultured as previously reported (87), in accordance with guidelines of Canton Vaud (Swiss animal experimentation authorization number VD1407.8).

Plasmids—All substrates used in this study were expressed from a pET21 plasmid containing an N-terminal methionine, the gene of interest, and a C-terminal FLAG tag. The plasmid pET21-APP-C83-FLAG, expressing the aa residues 688–770 of the 770-aa long isoform of APP, was generated according to the procedure described previously for the construction of the vector pET21-APP-C99-FLAG (88). The Notch-based substrate N100-FLAG contains the aa residues Val-1711 to Glu-1809 from mouse Notch1 ΔE (88). The PCR QuikChange site-directed mutagenesis kit (Stratagene, La Jolla, CA) and the template vector pET21-WT APP-C99-FLAG plasmid were used to

TABLE 1
Primers used for the generation of the recombinant APP-C99 substrates with mutations in the zinc binding residues His-6, His-13, His-14, and Lys-28
Fwd, forward; Rev, reverse.

Primers	Sequence (5′→3′)
H6A-Fwd	GAA-TTC-CGA-GCT-GAC-TCA-GGA-TAT-GAA-GTT-CA
H6A-Rev	TCC-TGA-GTC-AGC-TCG-GAA-TTC-TGC-ATC
H13A-Fwd	GGA-TAT-GAA-GTT-GCT-CAT-CAA-AAA-TTG-GTG-TTC-TTT-GC
H13A-Rev	CAA-TTT-TTG-ATG-AGC-AAC-TTC-ATA-TCC-TGA-GTC-ATG-TCG
H14A-Fwd	GAT-ATG-AAG-TTC-ATG-CTC-AAA-AAT-TGG-TGT-TCT-TTG-CAG
H14A-Rev	CAA-TTT-TTG-AGC-ATG-AAC-TTC-ATA-TCC-TGA-GTC-ATG-TCG
H13A/H14A-Fwd	GGA-TAT-GAA-GTT-GCT-GCT-CAA-AAA-TTG-GTG-TTC-TTT-GC
H13A/H14A-Rev	CAA-TTT-TTG-AGC-AGC-AAC-TTC-ATA-TCC-TGA-GTC
K28A-Fwd	GGG-TTC-AAA-CGC-AGG-TGC-AAT-CAT-TGG
K28A-Rev	TGA-TTG-CAC-CTG-CGT-TTG-AAC-CCA-C

generate all APP-C99-FLAG mutants used in this study: H6A, H13A, H14A, H6A/H13A, H6A/H14A, H13A/H14A, H6A/H13A/H14A, and K28A. The oligonucleotide primers containing the desired mutations were specifically purchased (Eurogentec, Liège, Belgium) as listed in Table 1. All mutants were verified by sequencing (Microsynth AG, Balgach, Switzerland) and are listed in Table 2.

Purification of γ-Secretase, APP-C83-FLAG, APP-C99-FLAG, and Notch-based N100-FLAG Substrates—γ-Secretase was purified by using CHO cells overexpressing γ-secretase and anti-FLAG M2 affinity resin (Sigma) as described previously (89). The recombinant γ-secretase substrates, WT APP-C99-FLAG (rAPP-C99), mutated APP-C99-FLAG, WT APP-C83-FLAG (rAPP-C83), and the analogous Notch-based N100-FLAG substrate (rNotch100) were overexpressed in *E. coli* strain BL21 and affinity-purified by using an anti-FLAG M2 affinity resin (Sigma) (89).

Cell-free γ-Secretase Activity Assays—In vitro γ-secretase assays using the WT and mutated recombinant substrates were performed as previously reported (90). Briefly, 1 μM WT or mutated APP-C99-FLAG, APP-C83-FLAG, or N100-FLAG substrates was added to purified γ-secretase, 0.025% phosphatidylethanolamine, and 0.10% phosphatidylcholine. After 4 h of incubation at 37 °C, all reactions were stopped by adding 0.5% SDS (final concentration), and the samples were further assayed by Western blotting analysis for the detection of AICD-FLAG, NICD-FLAG or Aβ, or by IP/MS for the detection of Aβ or AICD-FLAG (91, 92).

Immobilized Metal Affinity Chromatography—The Cu^{2+} ion affinity column was prepared by loading 20 mM $CuCl_2$ onto the prepacked immobilized iminodiacetic acid gel (from Pierce), which carries an iminodiacetic acid functional group to bind Cu^{2+}. The Cu^{2+} column and the control column (packed only with immobilized iminodiacetic acid gel) were washed and equilibrated with the binding buffer (0.25% CHAPSO in 20 mM Na_3PO_4, 0.5 M NaCl; pH 7). Next, binding assays were performed by loading microsomal preparations enriched in γ-secretase or highly purified γ-secretase preparations onto those columns. After washes with the binding buffer and preelution buffer (0.25% CHAPSO, 2 mM imidazole, 20 mM Na_3PO_4, 0.5 M NaCl; pH 7), bound proteins were collected with elution buffer (0.25% CHAPSO, 20 mM imidazole, 20 mM Na_3PO_4, 0.5 M NaCl; pH 7). Eluted fractions were used to detect γ-secretase subunits by Western blotting or to perform γ-secretase activity assays.

TABLE 2
List of recombinant APP-C99 mutants used as γ-secretase substrates in this study

Name	rAPP-C99 mutation
M1	H6A
M2	H13A
M3	H14A
M4	H6A/H13A
M5	H6A/H14A
M6	H13A/H14A
M7	H6A/H13A/H14A
M8	K28A

Western Blotting and Antibodies—For Western blotting analyses, samples from the *in vitro* γ-secretase activity assays were run on 4–12% Bis-tris gels (Invitrogen) and transferred onto PVDF membranes to detect the substrates APP-C99-FLAG, APP-C83-FLAG, and Notch-N100-FLAG and the cleavage products Aβ, AICD-FLAG, or NICD-FLAG. The FLAG-tagged substrates and the AICD-FLAG and NICD-FLAG products generated by γ-secretase proteolysis were detected with anti-FLAG M2 antibodies (1:1000, Sigma) and CT15 (1:5000, Sigma), whereas Aβ products were detected with 6E10 antibody (1:1000, Covance) and 4G8 (1:1000, Covance).

Statistical Analyses—All values are presented as the mean ± S.D. Statistical analyses were performed using an unpaired Student's *t*-test. *, $p < 0.05$; **, $p < 0.01$; ***, $p < 0.001$. $n = X$ indicates X independent experiments.

Method for Calculating IC_{50} Values—The IC_{50} values were estimated from a dose-response curve generated by plotting the logarithm-transformed Cu^{2+} or Zn^{2+} concentrations (x axis) and AICD/NICD/APP-CTFs/Aβ mean values estimated by densitometric analysis or by ELISA (y axis).

Blue Native Gel Electrophoresis—Purified γ-secretase or APP-based substrates were diluted in 0.1% CHAPSO-HEPES buffer and first incubated with Cu^{2+}, Zn^{2+}, DAPT, or H_2O (control) for 2 h at 37 °C. Next, 15 μl of the reactions were mixed with 6.25 μl of blue native sample buffer 4× (Invitrogen) and 3.75 μl of 5% G-250 sample additives (Invitrogen) and loaded onto a 4–16% blue native gel (Invitrogen), and proteins were resolved by blue native PAGE at 150 V for 30 min and then at 35 V for 2 h. Proteins were transferred onto a PVDF membrane and probed with an anti-nicastrin antibody (NCT164, 1:1000, BD Biosciences) for the detection of the γ-secretase complex or with an anti-FLAG antibody (M2, 1:1000, Sigma) for the detection of APP-C99-FLAG.

IP/MS Analysis of Aβ and AICD—IP/MS was performed as described previously (91, 92). Briefly, triplicate samples from *in*

vitro γ-secretase activity assays were pooled and incubated overnight at 4 °C with 2.5 μl of the antibody 4G8 (1:1000, Covance) and 30 μl of protein G (Sigma) to precipitate Aβ. For the IP of AICD-FLAG, samples were treated for 20 min at 55 °C with Triton X-100 (1%) before overnight IP at 4 °C with the anti-FLAG M2 affinity gel (Sigma). After IP, the beads were washed 3 times with washing buffer (50 mM HEPES, 150 mM NaCl, and 0.1% *n*-octyl-β-D-glycopyranoside; pH 7.4), and IPed proteins were eluted with trifluoroacetic acid (1%):acetonitrile:H_2O (1:20:20). The elution was then equally mixed with saturated α-cyano-4-hydroxycinnamic acid or sinapic acid for the respective analysis by MALDI-MS of Aβ (in reflectron mode) and of AICD (in linear mode).

Author Contributions—F. W. generated Figs. 1*B*, 1*C*, 2*C*, 2*D*, 3, *A–F*, and 5. M. D. generated Figs. 2*E*, 4*D*, and 4*E*. G. M. G. O. generated Figs. 4*A* and 4*B*. H. G. performed all other experiments described in Figs. 1–8. P. C. F. and F. W. initiated the project. P. C. F. supervised the project and provided funding. H. G., F. W., M. D., and P. C. F. wrote the manuscript. All authors edited the manuscript.

Acknowledgments—We thank D. Selkoe (Harvard Medical School and Brigham and Woman's Hospital, Boston, MA) for the γ-30 cell line, J. Puyal and V. Ginet (University of Lausanne, Switzerland) for help with primary cortical neurons, and U. Albrecht (University of Fribourg, Switzerland) for helpful discussions.

References

1. Barker, W. W., Luis, C. A., Kashuba, A., Luis, M., Harwood D. G., Loewenstein, D., Waters, C., Jimison, P., Shepherd, E., Sevush, S., Graff-Radford, N., Newland, D., Todd, M., Miller, B., Gold, M., et al. (2002) Relative frequencies of Alzheimer's disease, Lewy body, vascular and frontotemporal dementia, and hippocampal sclerosis in the State of Florida Brain Bank. *Alzheimer Dis. Assoc, Disord.* **16,** 203–212
2. Jakob-Roetne, R., and Jacobsen, H. (2009) Alzheimer's disease: from pathology to therapeutic approaches. *Angew. Chem. Int. Ed. Engl.* **48,** 3030–3059
3. Cummings, J. L., Morstorf, T., and Zhong, K. (2014) Alzheimer's disease drug-development pipeline: few candidates, frequent failures. *Alzheimers Res. Ther.* **6,** 37
4. Lovell, M. A., Robertson, J. D., Teesdale, W. J., Campbell, J. L., and Markesbery, W. R. (1998) Copper, iron, and zinc in Alzheimer's disease senile plaques. *J. Neurol. Sci.* **158,** 47–52
5. Pithadia, A. S., and Lim, M. H. (2012) Metal-associated amyloid-β species in Alzheimer's disease. *Curr. Opin. Chem. Biol.* **16,** 67–73
6. Assaf, S. Y., and Chung, S. H. (1984) Release of endogenous Zn^{2+} from brain tissue during activity. *Nature* **308,** 734–736
7. Hartter, D. E., and Barnea, A. (1988) Evidence for release of copper in the brain: depolarization-induced release of newly taken-up 67copper. *Synapse* **2,** 412–415
8. Kardos, J., Kovács, I., Hajós, F., Kálmán, M., and Simonyi, M. (1989) Nerve endings from rat brain tissue release copper upon depolarization: a possible role in regulating neuronal excitability. *Neurosci. Lett.* **103,** 139–144
9. Schlief, M. L., Craig, A. M., and Gitlin, J. D. (2005) NMDA receptor activation mediates copper homeostasis in hippocampal neurons. *J. Neurosci.* **25,** 239–246
10. Faller, P., and Hureau, C. (2009) Bioinorganic chemistry of copper and zinc ion coordinated to amyloid-β peptide. *Dalton Trans.* **7,** 1080–1094 (10.1039/b813398k)
11. Hesse, L., Beher, D., Masters, C. L., and Multhaup, G. (1994) The βA4 amyloid precursor protein binding to copper. *FEBS Lett.* **349,** 109–116
12. Bush, A. I., Multhaup, G., Moir, R. D., Williamson, T. G., Small, D. H., Rumble, B., Pollwein, P., Beyreuther, K., and Masters, C. L. (1993) A novel zinc(II) binding site modulates the function of the βA4 amyloid protein precursor of Alzheimer's disease. *J. Biol. Chem.* **268,** 16109–16112
13. Miller, Y., Ma, B., and Nussinov, R. (2010) Zinc ions promote Alzheimer Aβ aggregation via population shift of polymorphic states. *Proc. Natl. Acad. Sci.* **107,** 9490–9495
14. Treiber, C., Simons, A., Strauss, M., Hafner, M., Cappai, R., Bayer, T. A., and Multhaup, G. (2004) Clioquinol mediates copper uptake and counteracts copper efflux activities of the amyloid precursor protein of Alzheimer's disease. *J. Biol. Chem.* **279,** 51958–51964
15. Maynard, C. J., Cappai, R., Volitakis, I., Cherny, R. A., White, A. R., Beyreuther, K., Masters, C. L., Bush, A. I., and Li, Q.-X. (2002) Overexpression of Alzheimer's disease amyloid-β opposes the age-dependent elevations of brain copper and iron. *J. Biol. Chem.* **277,** 44670–44676
16. Bellingham, S. A., Ciccotosto, G. D., Needham, B. E., Fodero, L. R., White, A. R., Masters, C. L., Cappai, R., and Camakaris, J. (2004) Gene knockout of amyloid precursor protein and amyloid precursor-like protein-2 increases cellular copper levels in primary mouse cortical neurons and embryonic fibroblasts. *J. Neurochem.* **91,** 423–428
17. Crouch, P. J., Hung, L. W., Adlard, P. A., Cortes, M., Lal, V., Filiz, G., Perez, K. A., Nurjono, M., Caragounis, A., Du, T., Laughton, K., Volitakis, I., Bush, A. I., Li, Q.-X., Masters, C. L., *et al.* (2009) Increasing Cu bioavailability inhibits Aβ oligomers and tau phosphorylation. *Proc. Natl. Acad. Sci. U.S.A.* **106,** 381–386
18. Phinney, A. L., Drisaldi, B., Schmidt, S. D., Lugowski, S., Coronado, V., Liang, Y., Horne, P., Yang, J., Sekoulidis, J., Coomaraswamy, J., Chishti, M. A., Cox, D. W., Mathews, P. M., Nixon, R. A., Carlson, G. A., *et al.* (2003) *In vivo* reduction of amyloid-β by a mutant copper transporter. *Proc. Natl. Acad. Sci.* **100,** 14193–14198
19. Hung, Y. H., Bush, A. I., and Cherny, R. A. (2010) Copper in the brain and Alzheimer's disease. *J. Biol. Inorg. Chem.* **15,** 61–76
20. Adlard, P. A., Cherny, R. A., Finkelstein, D. I., Gautier, E., Robb, E., Cortes, M., Volitakis, I., Liu, X., Smith, J. P., Perez, K., Laughton, K., Li, Q.-X., Charman, S. A., Nicolazzo, J. A., Wilkins, S., *et al.* (2008) Rapid restoration of cognition in Alzheimer's transgenic mice with 8-hydroxy quinoline analogs is associated with decreased interstitial Aβ. *Neuron* **59,** 43–55
21. Lannfelt, L., Blennow, K., Zetterberg, H., Batsman, S., Ames, D., Harrison, J., Masters, C. L., Targum, S., Bush, A. I., Murdoch, R., Wilson, J., Ritchie, C. W., and PBT2–201-EURO study group. (2008) Safety, efficacy, and biomarker findings of PBT2 in targeting Aβ as a modifying therapy for Alzheimer's disease: a phase IIa, double-blind, randomised, placebo-controlled trial. *Lancet Neurol.* **7,** 779–786
22. Adlard, P. A., Parncutt, J. M., Finkelstein, D. I., and Bush, A. I. (2010) Cognitive loss in zinc transporter-3 knock-out mice: a phenocopy for the synaptic and memory deficits of Alzheimer's disease? *J. Neurosci.* **30,** 1631–1636
23. Donnelly, P. S., Caragounis, A., Du, T., Laughton, K. M., Volitakis, I., Cherny, R. A., Sharples, R. A., Hill, A. F., Li, Q.-X., Masters, C. L., Barnham, K. J., and White, A. R. (2008) Selective intracellular release of copper and zinc ions from bis(thiosemicarbazonato) complexes reduces levels of Alzheimer disease amyloid-β peptide. *J. Biol. Chem.* **283,** 4568–4577
24. Hung, Y. H., Robb, E. L., Volitakis, I., Ho, M., Evin, G., Li, Q.-X., Culvenor, J. G., Masters, C. L., Cherny, R. A., and Bush, A. I. (2009) Paradoxical condensation of copper with elevated β-amyloid in lipid rafts under cellular copper deficiency conditions. *J. Biol. Chem.* **284,** 21899–21907
25. Kaether, C., Lammich, S., Edbauer, D., Ertl, M., Rietdorf, J., Capell, A., Steiner, H., and Haass, C. (2002) Presenilin-1 affects trafficking and processing of βAPP and is targeted in a complex with nicastrin to the plasma membrane. *J. Cell Biol.* **158,** 551–561
26. Chyung, J. H., Raper, D. M., and Selkoe, D. J. (2005) γ-Secretase exists on the plasma membrane as an intact complex that accepts substrates and effects intramembrane cleavage. *J. Biol. Chem.* **280,** 4383–4392
27. Wang, Y., Hodgkinson, V., Zhu, S., Weisman, G. A., and Petris, M. J. (2011) Advances in the understanding of mammalian copper transporters. *Adv. Nutr.* **2,** 129–137
28. Camakaris, J., Voskoboinik, I., and Mercer, J. F. (1999) Molecular mechanisms of copper homeostasis. *Biochem. Biophys. Res. Commun.* **261,** 225–232

29. Takeda, A., Sakurada, N., Ando, M., Kanno, S., and Oku, N. (2009) Facilitation of zinc influx via AMPA/kainate receptor activation in the hippocampus. *Neurochem. Int.* **55,** 376–382
30. Li, Y., Hough, C. J., Suh, S. W., Sarvey, J. M., and Frederickson, C. J. (2001) Rapid translocation of Zn^{2+} from presynaptic terminals into postsynaptic hippocampal neurons after physiological stimulation. *J. Neurophysiol.* **86,** 2597–2604
31. Borchardt, T., Camakaris, J., Cappai, R., Masters, C. L., Beyreuther, K., and Multhaup, G. (1999) Copper inhibits β-amyloid production and stimulates the non-amyloidogenic pathway of amyloid-precursor-protein secretion. *Biochem. J.* **344,** 461–467
32. Cater, M. A., McInnes, K. T., Li, Q.-X., Volitakis, I., La Fontaine, S., Mercer, J. F., and Bush, A. I. (2008) Intracellular copper deficiency increases amyloid-β secretion by diverse mechanisms. *Biochem. J.* **412,** 141–152
33. Acevedo, K. M., Hung, Y. H., Dalziel, A. H., Li, Q.-X., Laughton, K., Wikhe, K., Rembach, A., Roberts, B., Masters, C. L., Bush, A. I., and Camakaris, J. (2011) Copper promotes the trafficking of the amyloid precursor protein. *J. Biol. Chem.* **286,** 8252–8262
34. Minicozzi, V., Stellato, F., Comai, M., Dalla Serra, M., Potrich, C., Meyer-Klaucke, W., and Morante, S. (2008) Identifying the minimal copper- and zinc-binding site sequence in amyloid-β peptides. *J. Biol. Chem.* **283,** 10784–10792
35. Fraering, P. C. (2007) Structural and Functional Determinants of γ-secretase, an intramembrane protease implicated in Alzheimer's disease. *Curr. Genomics* **8,** 531–549
36. Cacquevel, M., Aeschbach, L., Osenkowski, P., Li, D., Ye, W., Wolfe, M. S., Li, H., Selkoe, D. J., and Fraering, P. C. (2008) Rapid purification of active γ-secretase, an intramembrane protease implicated in Alzheimer's disease. *J. Neurochem.* **104,** 210–220
37. Fraering, P. C., LaVoie, M. J., Ye, W., Ostaszewski, B. L., Kimberly, W. T., Selkoe, D. J., and Wolfe, M. S. (2004) Detergent-dependent dissociation of active γ-secretase reveals an interaction between Pen-2 and PS1-NTF and offers a model for subunit organization within the complex. *Biochemistry* **43,** 323–333
38. Alvarez, H. M., Xue, Y., Robinson, C. D., Canalizo-Hernández, M. A., Marvin, R. G., Kelly, R. A., Mondragón, A., Penner-Hahn, J. E., and O'Halloran, T. V. (2010) Tetrathiomolybdate inhibits copper trafficking proteins through metal cluster formation. *Science* **327,** 331–334
39. Quagraine, E. K., Kraatz, H. B., and Reid, R. S. (2001) Peptides mimicking the N-terminal Cu(II)-binding site of bovine serum albumin: synthesis, characterization and coordination with Cu(II) ions. *J. Inorg. Biochem.* **85,** 23–32
40. She, Y.-M., Narindrasorasak, S., Yang, S., Spitale, N., Roberts, E. A., and Sarkar, B. (2003) Identification of metal-binding proteins in human hepatoma lines by immobilized metal affinity chromatography and mass spectrometry. *Mol. Cell. Proteomics* **2,** 1306–1318
41. Roberts, S. A., Wildner, G. F., Grass, G., Weichsel, A., Ambrus, A., Rensing, C., and Montfort, W. R. (2003) A labile regulatory copper ion lies near the T1 copper site in the multicopper oxidase CueO. *J. Biol. Chem.* **278,** 31958–31963
42. Takahashi, Y., Kako, K., Kashiwabara, S.-I., Takehara, A., Inada, Y., Arai, H., Nakada, K., Kodama, H., Hayashi, J.-I., Baba, T., and Munekata, E. (2002) Mammalian copper chaperone Cox17p has an essential role in activation of cytochrome *c* oxidase and embryonic development. *Mol. Cell. Biol.* **22,** 7614–7621
43. Welander, H., Frånberg, J., Graff, C., Sundström, E., Winblad, B., and Tjernberg, L. O. (2009) Aβ43 is more frequent than Aβ40 in amyloid plaque cores from Alzheimer disease brains. *J. Neurochem.* **110,** 697–706
44. Sandebring, A., Welander, H., Winblad, B., Graff, C., and Tjernberg, L. O. (2013) The pathogenic aβ43 is enriched in familial and sporadic Alzheimer disease. *PloS ONE* **8,** e55847
45. Mithu, V. S., Sarkar, B., Bhowmik, D., Chandrakesan, M., Maiti, S., and Madhu, P. K. (2011) Zn^{2+} binding disrupts the Asp- 23–Lys-28 salt bridge without altering the hairpin-shaped cross-β structure of Aβ42 amyloid aggregates. *Biophys. J.* **101,** 2825–2832
46. Kukar, T. L., Ladd, T. B., Robertson, P., Pintchovski, S. A., Moore, B., Bann, M. A., Ren, Z., Jansen-West, K., Malphrus, K., Eggert, S., Maruyama, H., Cottrell, B. A., Das, P., Basi, G. S., Koo, E. H., and Golde, T. E. (2011) Lysine 624 of the amyloid precursor protein (APP) is a critical determinant of amyloid β peptide length: support for a sequential model of γ-secretase intramembrane proteolysis and regulation by the amyloid β precursor protein (APP) juxtamembrane region. *J. Biol. Chem.* **286,** 39804–39812
47. Page, R. M., Gutsmiedl, A., Fukumori, A., Winkler, E., Haass, C., and Steiner, H. (2010) β-Amyloid precursor protein mutants respond to γ-secretase modulators. *J. Biol. Chem.* **285,** 17798–17810
48. Bush, A. (2013) The metal theory of Alzheimer's disease. *J. Alzheimers Dis.* **33,** S277–S281
49. Hung, Y. H., Bush, A. I., and La Fontaine, S. (2013) Links between copper and cholesterol in Alzheimer's disease. *Front. Physiol.* **4,** 111
50. Noda, Y., Asada, M., Kubota, M., Maesako, M., Watanabe, K., Uemura, M., Kihara, T., Shimohama, S., Takahashi, R., Kinoshita, A., and Uemura, K. (2013) Copper enhances APP dimerization and promotes Aβ production. *Neurosci. Lett.* **547,** 10–15
51. James, S. A., Volitakis, I., Adlard, P. A., Duce, J. A., Masters, C. L., Cherny, R. A., and Bush, A. I. (2012) Elevated labile Cu is associated with oxidative pathology in Alzheimer disease. *Free Radic. Biol. Med.* **52,** 298–302
52. Bonda, D. J., Lee, H. G., Blair, J. A., Zhu, X., Perry, G., and Smith, M. A. (2011) Role of metal dyshomeostasis in Alzheimer's disease. *Metallomics* **3,** 267–270
53. Schlief, M. L., West, T., Craig, A. M., Holtzman, D. M., and Gitlin, J. D. (2006) Role of the Menkes copper-transporting ATPase in NMDA receptor-mediated neuronal toxicity. *Proc. Natl. Acad. Sci. U.S.A.* **103,** 14919–14924
54. Butterfield, D. A., and Pocernich, C. B. (2003) The glutamatergic system and Alzheimer's disease: therapeutic implications. *CNS Drugs* **17,** 641–652
55. Zhou, L.-X., Du, J.-T., Zeng, Z.-Y., Wu, W.-H., Zhao, Y.-F., Kanazawa, K., Ishizuka, Y., Nemoto, T., Nakanishi, H., and Li, Y.-M. (2007) Copper (II) modulates *in vitro* aggregation of a tau peptide. *Peptides* **28,** 2229–2234
56. Soragni, A., Zambelli, B., Mukrasch, M. D., Biernat, J., Jeganathan, S., Griesinger, C., Ciurli, S., Mandelkow, E., and Zweckstetter, M. (2008) Structural characterization of binding of Cu(II) to tau protein. *Biochemistry* **47,** 10841–10851
57. Arnal, N., Morel, G. R., de Alaniz, M. J., Castillo, O., and Marra, C. A. (2013) Role of copper and cholesterol association in the neurodegenerative process. *Int. J. Alzheimers Dis.* **2013,** 414817
58. Jun, S., and Saxena, S. (2007) The aggregated state of amyloid-β peptide *in vitro* depends on Cu^{2+} ion concentration. *Angew. Chem. Int. Ed. Engl.* **46,** 3959–3961
59. Ha, C., Ryu, J., and Park, C. B. (2007) Metal ions differentially influence the aggregation and deposition of Alzheimer's β-amyloid on a solid template. *Biochemistry* **46,** 6118–6125
60. Yoon, K., and Gaiano, N. (2005) Notch signaling in the mammalian central nervous system: insights from mouse mutants. *Nat. Neurosci.* **8,** 709–715
61. Wines-Samuelson, M., and Shen, J. (2005) Presenilins in the developing, adult, and aging cerebral cortex. *Neuroscientist* **11,** 441–451
62. Saura, C. A., Choi, S.-Y., Beglopoulos, V., Malkani, S., Zhang, D., Shankaranarayana Rao, B. S., Chattarji, S., Kelleher, R. J., 3rd, Kandel, E. R., Duff, K., Kirkwood, A., and Shen, J. (2004) Loss of presenilin function causes impairments of memory and synaptic plasticity followed by age-dependent neurodegeneration. *Neuron.* **42,** 23–36
63. Costa, R. M., Honjo, T., and Silva, A. J. (2003) Learning and memory deficits in Notch mutant mice. *Curr. Biol.* **13,** 1348–1354
64. Wang, Y., Chan, S. L., Miele, L., Yao, P. J., Mackes, J., Ingram, D. K., Mattson, M. P., and Furukawa, K. (2004) Involvement of Notch signaling in hippocampal synaptic plasticity. *Proc. Natl. Acad. Sci. U.S.A.* **101,** 9458–9462
65. Kim, D., and Tsai, L.-H. (2009) Bridging physiology and pathology in AD. *Cell* **137,** 997–1000
66. Alattia, J.-R., Kuraishi, T., Dimitrov, M., Chang, I., Lemaitre, B., and Fraering, P. C. (2011) Mercury is a direct and potent γ-secretase inhibitor affecting Notch processing and development in *Drosophila*. *FASEB J.* **25,** 2287–2295
67. Bot, N., Schweizer, C., Ben Halima, S., and Fraering, P. C. (2011) Processing of the synaptic cell adhesion molecule neurexin-3β by Alzheimer disease α- and γ-secretases. *J. Biol. Chem.* **286,** 2762–2773

68. Doody, R. S., Raman, R., Farlow, M., Iwatsubo, T., Vellas, B., Joffe, S., Kieburtz, K., He, F., Sun, X., Thomas, R. G., Aisen, P. S., Alzheimer's Disease Cooperative Study Steering Committee, Siemers, E., Sethuraman, G., Mohs, R., and Semagacestat Study Group. (2013) A phase 3 trial of semagacestat for treatment of Alzheimer's disease. *N. Engl. J. Med.* **369,** 341–350
69. Brewer, G. J. (2000) Recognition, diagnosis, and management of Wilson's disease. *Proc. Soc. Exp. Biol. Med.* **223,** 39–46
70. Squitti, R., and Polimanti, R. (2012) Copper hypothesis in the missing hereditability of sporadic Alzheimer's disease: ATP7B gene as potential harbor of rare variants. *J. Alzheimers Dis.* **29,** 493–501
71. Bush, A. I., and Tanzi, R. E. (2008) Therapeutics for Alzheimer's disease based on the metal hypothesis. *Neurotherapeutics* **5,** 421–432
72. Kenche, V. B., and Barnham, K. J. (2011) Alzheimer's disease and metals: therapeutic opportunities. *Br. J. Pharmacol.* **163,** 211–219
73. Ayton, S., Lei, P., and Bush, A. I. (2015) Biometals and their therapeutic implications in Alzheimer's disease. *Neurotherapeutics* **12,** 109–120
74. Ritchie, C. W., Bush, A. I., Mackinnon, A., Macfarlane, S., Mastwyk, M., MacGregor, L., Kiers, L., Cherny, R., Li, Q.-X., Tammer, A., Carrington, D., Mavros, C., Volitakis, I., Xilinas, M., Ames, D., *et al.* (2003) Metal-protein attenuation with iodochlorhydroxyquin (clioquinol) targeting Aβ amyloid deposition and toxicity in Alzheimer disease: a pilot phase 2 clinical trial. *Arch. Neurol.* **60,** 1685–1691
75. Faux, N. G., Ritchie, C. W., Gunn, A., Rembach, A., Tsatsanis, A., Bedo, J., Harrison, J., Lannfelt, L., Blennow, K., Zetterberg, H., Ingelsson, M., Masters, C. L., Tanzi, R. E., Cummings, J. L., Herd, C. M., and Bush, A. I. (2010) PBT2 rapidly improves cognition in Alzheimer's Disease: additional phase II analyses. *J. Alzheimers Dis.* **20,** 509–516
76. Squitti, R., Siotto, M., and Polimanti, R. (2014) Low-copper diet as a preventive strategy for Alzheimer's disease. *Neurobiol. Aging.* **35,** S40–S50
77. Boukaïba, N., Flament, C., Acher, S., Chappuis, P., Piau, A., Fusselier, M., Dardenne, M., and Lemonnier, D. (1993) A physiological amount of zinc supplementation: effects on nutritional, lipid, and thymic status in an elderly population. *Am. J. Clin. Nutr.* **57,** 566–572
78. Cole, T. B., Wenzel, H. J., Kafer, K. E., Schwartzkroin, P. A., and Palmiter, R. D. (1999) Elimination of zinc from synaptic vesicles in the intact mouse brain by disruption of the ZnT3 gene. *Proc. Natl. Acad. Sci. U.S.A.* **96,** 1716–1721
79. Strozyk, D., Launer, L. J., Adlard, P. A., Cherny, R. A., Tsatsanis, A., Volitakis, I., Blennow, K., Petrovitch, H., White, L. R., and Bush, A. I. (2009) Zinc and copper modulate Alzheimer Aβ levels in human cerebrospinal fluid. *Neurobiol. Aging* **30,** 1069–1077
80. Hoke, D. E., Tan, J.-L., Ilaya, N. T., Culvenor, J. G., Smith, S. J., White, A. R., Masters, C. L., and Evin, G. M. (2005) *In vitro* γ-secretase cleavage of the Alzheimer's amyloid precursor protein correlates to a subset of presenilin complexes and is inhibited by zinc. *FEBS J.* **272,** 5544–5557
81. Winkler, E., Julius, A., Steiner, H., and Langosch, D. (2015) Homodimerization protects the amyloid precursor protein C99 fragment from cleavage by γ-secretase. *Biochemistry* **54,** 6149–6152
82. Danielsson, J., Pierattelli, R., Banci, L., and Gräslund, A. (2007) High-resolution NMR studies of the zinc-binding site of the Alzheimer's amyloid β-peptide. *FEBS J.* **274,** 46–59
83. Takami, M., Nagashima, Y., Sano, Y., Ishihara, S., Morishima-Kawashima, M., Funamoto, S., and Ihara, Y. (2009) γ-Secretase: successive tripeptide and tetrapeptide release from the transmembrane domain of β-carboxyl terminal fragment. *J. Neurosci.* **29,** 13042–13052
84. Kukar, T. L., Ladd, T. B., Bann, M. A., Fraering, P. C., Narlawar, R., Maharvi, G. M., Healy, B., Chapman, R., Welzel, A. T., Price, R. W., Moore, B., Rangachari, V., Cusack, B., Eriksen, J., Jansen-West, K., *et al.* (2008) Substrate-targeting γ-secretase modulators. *Nature* **453,** 925–929
85. Houacine, J., Bolmont, T., Aeschbach, L., Oulad-Abdelghani, M., and Fraering, P. C. (2012) Selective neutralization of APP-C99 with monoclonal antibodies reduces the production of Alzheimer's Aβ peptides. *Neurobiol. Aging* **33,** 2704–2714
86. Cacquevel, M., Aeschbach, L., Houacine, J., and Fraering, P. C. (2012) Alzheimer's disease-linked mutations in presenilin-1 result in a drastic loss of activity in purified γ-secretase complexes. *PloS ONE* **7,** e35133
87. Ginet, V., Spiehlmann, A., Rummel, C., Rudinskiy, N., Grishchuk, Y., Luthi-Carter, R., Clarke, P. G., Truttmann, A. C., and Puyal, J. (2014) Involvement of autophagy in hypoxic-excitotoxic neuronal death. *Autophagy* **10,** 846–860
88. Esler, W. P., Kimberly, W. T., Ostaszewski, B. L., Ye, W., Diehl, T. S., Selkoe, D. J., and Wolfe, M. S. (2002) Activity-dependent isolation of the presenilin-γ-secretase complex reveals nicastrin and a γ substrate. *Proc. Natl. Acad. Sci.* **99,** 2720–2725
89. Fraering, P. C., Ye, W., LaVoie, M. J., Ostaszewski, B. L., Selkoe, D. J., and Wolfe, M. S. (2005) γ-Secretase substrate selectivity can be modulated directly via interaction with a nucleotide-binding site. *J. Biol. Chem.* **280,** 41987–41996
90. Wu, F., Schweizer, C., Rudinskiy, N., Taylor, D. M., Kazantsev, A., Luthi-Carter, R., and Fraering, P. C. (2010) Novel γ-secretase inhibitors uncover a common nucleotide-binding site in JAK3, SIRT2, and PS1. *FASEB J.* **24,** 2464–2474
91. Dimitrov, M., Alattia, J.-R., Lemmin, T., Lehal, R., Fligier, A., Houacine, J., Hussain, I., Radtke, F., Dal Peraro, M., Beher, D., and Fraering, P. C. (2013) Alzheimer's disease mutations in APP but not γ-secretase modulators affect epsilon-cleavage-dependent AICD production. *Nat. Commun.* **4,** 2246
92. Ayciriex, S., Gerber, H., Osuna, G. M., Chami, M., Stahlberg, H., Shevchenko, A., and Fraering, P. C. (2016) The lipidome associated with the γ-secretase complex is required for its integrity and activity. *Biochem. J.* **473,** 321–334